

國立交通大學
生化工程研究所
碩士論文

利用不同來源醯亞胺水解酵素之受質特異性及
金屬含量之差異探討其催化機制



**From the Substrate Specificity and Metal Content of Various
imidases to deduce the Catalytic Mechanism and Action**

研究生：張淑婷

指導教授：楊裕雄教授

中華民國九十五年六月

利用不同來源醯亞胺水解酵素之受質特異性及

金屬含量之差異探討其催化機制

學生：張淑婷

指導教授：楊裕雄 博士

國立交通大學生化工程研究所碩士班

摘要

醯亞胺水解酵素(imidase) 是一個廣效性的解毒酵素，能催化含有醯亞胺官能基的化合物，然而其特異性與催化機制一直不了解，尤其是不同來源的醯亞胺水解酵素更有著顯著的差異。在此我們利用 LC-ESI-MS 證實從魚肝中純化取得之酵素為醯亞胺水解酵素，並在取得序列之後利用 Homology Modeling 及 GOLD Docking 電腦模擬之方式探討金屬含量之差異在催化機制扮演的角色。分析 GOLD 及酵素實驗的結果顯示，5-hydantoin acetic acid 及 Parabanic acid 對細菌性醯亞胺水解酵素為受質，然而，對魚類醯亞胺水解酵素則是競爭型抑制劑。GOLD 的模擬結果顯示，相較於細菌性醯亞胺水解酵素具有兩個金屬（位於 α -site 及 β -site），魚類醯亞胺水解酵素只具有一個位於 α -site 之金屬，因此空出的 β -site 及 K148, H187, H243 便可與化合物形成氫鍵並使其位向偏向 β -site。

From the Substrate Specificity and Metal Content of Various Imidases to deduce the Catalytic Mechanism and Action

Student : Shu-Ting Chang

Advisors : Dr. Yuh-Shyong Yang

Institute of Biochemical Engineering, College of Biological Science and
Technology, National Chiao Tung University, Hsinchu, Taiwan, ROC.



ABSTRACT

Imidase catalyzes hydrolysis of many imides. Significant variations are found in sequence and metal content for imidases from different organisms that catalyze similar reactions. In this study, LC-ESI-MS results indicated that the purified enzyme from fish liver is imidase. The nucleotide sequence of fish imidase was obtained. Then homology modeling and molecular docking were used to study about the different number of metals in the different species. Molecular docking of 5-hydantoinacetic acid and parabanic acid into fish imidase showed that both of them can enter the active site, but had different orientations than those in hydantoinase. Enzymatic assays showed that bacterial hydantoinase hydrolyzed the 5-hydantoinacetic acid and parabanic acid, however, the two compounds were competitive inhibitors for fish imidase. A reasonable explanation is that fish imidase has the only zinc in the α - site. 5-hydantoinacetic acid and parabanic acid entered the active site, they tended to the open β -site and formed weak hydrogen bonds with free residues, K154, H187 and H243.

ACKNOWLEDGEMENT

兩年的碩班生活十分的辛苦，但也讓我獲益良多，這一路跌跌撞撞走來，要感謝許多人，首先要感謝我的指導教授楊裕雄老師，老師給予我們許多獨立思考的空間，也讓我們能夠做許多嘗試與挑戰，在這樣的環境下讓我成長了許多另外，也要感謝簡慶德老師，張家靖老師，以及許鈺宗老師能擔任我的口試委員，對於我的論文給予了許多指導與建議。

LEPE 這一個大家族的每一個成員也都是我要感謝的，Rich 學長、郁吟學姊、大晃學長、僕僕學長、陸宜總是在我遇到困難時給予我許多建議，還有我的同學嘉蔚、小志、昱樹、peggy，恭喜大家一起畢業了，另外還有美春、小丸、淵仁學長、蕙菁學姊、jumping、來姐、政哲學長、莊博，謝謝大家的照顧。

最後，要感謝我的家人，給了我最大的支持，讓我終於完成了碩班學業。



Contents	
Abstract (Chinese)	i
Abstract (English)	ii
Acknowledgement	iii
Contents	iv
Content of table and figure	v
Abbreviations and Symbols	vi
Chapter 1	Introduction1
1. 1	Biological importance of imidase1
1. 2	Industrial application of hydantoinase5
1. 3	Properties of imidase7
Chapter 2	Experimental procedures15
2. 1	Materials.....15
2. 2	Enzyme standard assay.....15
2. 3	Protein concentration.....15
2. 4	Protein purification16
2. 5	In gel digestion and identification using LC-ESI-MS..... 17
2. 6	RNA extraction and cDNA synthesis.....18
2. 7	PCR cloning and sequencing18
2. 8	Sequence analysis.....18
2. 9	Homology Modeling and Molecular Docking.....19
2. 10	Inhibition assay.....19
2. 11	Analysis of Kinetics Data.....19
Chapter 3	Results and discussion20
3. 1	Purification of fish liver imidase20
3. 2	Identification of fish liver imidase20
3. 3	Cloning of fish liver imidase21
3. 4	Homology Modeling and Generation of the active site structure.....21
3. 5	Molecular Docking.....23
3. 6	Proposed catalytic mechanism of fish liver imidase.....24
Chapter 4	Conclusions25
Reference	26
Appendix	50

Content of table and figure

Table 1	Summary of purification of imidase from fish liver	37
Table 2	Rate constants of various imidases using 5-Hydantoinacetic acid and Parabanic acid as substrate.....	48
Table 3	Inhibitory Activities of 5-Hydantoinacetic acid and Parabanic acid.....	49
Figure 1	The purity of fish liver imidase	38
Figure 2	fish liver imidase was analyzed using LC-ESI-MS.....	39
Figure 3	Sequence alignment of various imidase correlated with the sequence database by Mascot software	40
Figure 4	Nucleotide sequence and deduced amino acid sequence.....	42
Figure 5	Sequence alignment	43
Figure 6	Sequence alignment	44
Figure 7	Homology Modeling.....	45
Figure 8	GOLD modeling of 5-hydantoinacetic acid binding.....	46
Figure 9	GOLD modeling of parabanic acid binding	47



Abbreviation and symbol	Full Name
ICP-MS	Inductively coupled plasma-mass spectrometry
EDTA	(ethylenedinitrilo) tetracetic acid
Bis-Tris-propane	1,3-bis(tris(hydroxymethyl)methylamino)propane
Tris-HCl	tris(hydroxymethyl)aminomethane hydrochloride
DEAE	diethylaminoethyl
SDS	sodium dodecyl sulfate
PAGE	polyacrylamide gel electrophoresis
PMSF	phenylmethylsulfonyl fluoride
kDa	Kilodalton
K _m	Michaelis constant
K _i	Inhibitory constant
V _{max}	Maximum velocity



1. Introduction

1.1 Biological importance of imidase

Imidase is an enzyme that catalyzes the hydrolytic cleavage of imides that range from the linear to the heterocyclic and that include hydantoins, dihydropyrimidines, and phthalimide (Yang et al. 1993). Due to its broad substrate specificity, imidase is also known as dihydropyrimidinase (EC 3.5.2.2), dihydropyrimidine hydrase, dihydropyrimidine amidohydrolase and hydantoinase (Yang et al. 1993). The typical reactions catalyzed by imidase are summarized as shown in Figure 1.

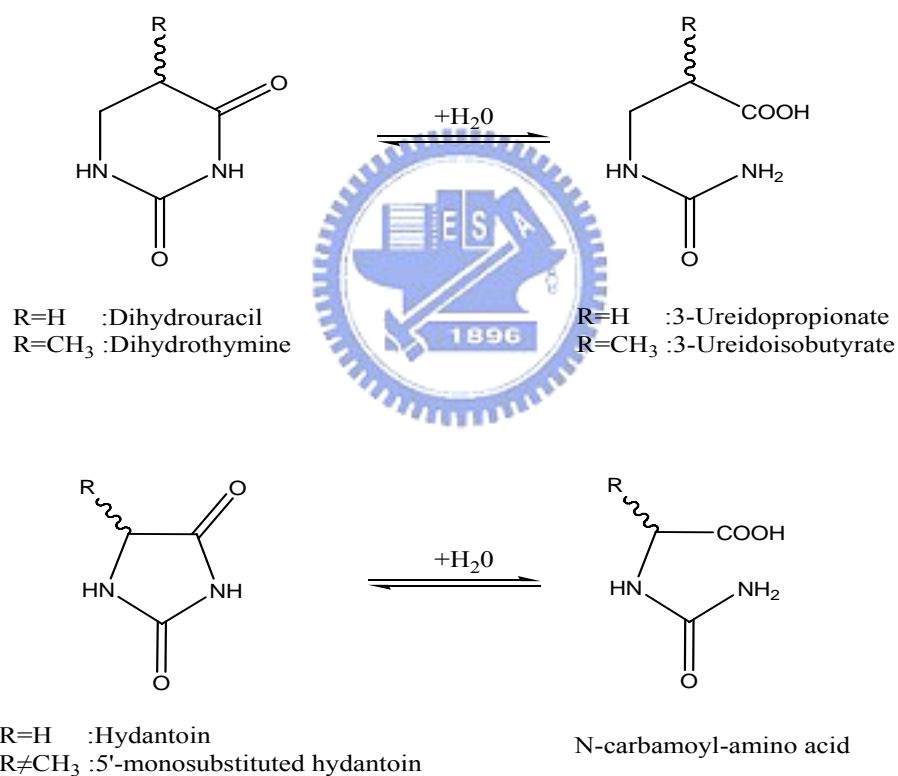


Figure 1. The typical reactions catalyzed by imidase.

Imide-hydrolyzing enzymes were first described in the 1940's. The enzymes were widely distributed in living organisms such as plants (Eadie et al., 1949) and animals (Bernheim and Bernheim, 1946). In the 1950's, an imide-hydrolyzing enzyme isolated from calf liver was

shown occurring in the metabolism of pyrimidines and thus was classified as dihydropyrimidinase (Wallach and Grisolia, 1957). This was a first attempt to characterize some properties of the partially purified enzyme from animals and discovered that dihydropyrimidinase used dihydropyrimidine (dihydrouracil and dihydrothymine) as natural substrate.

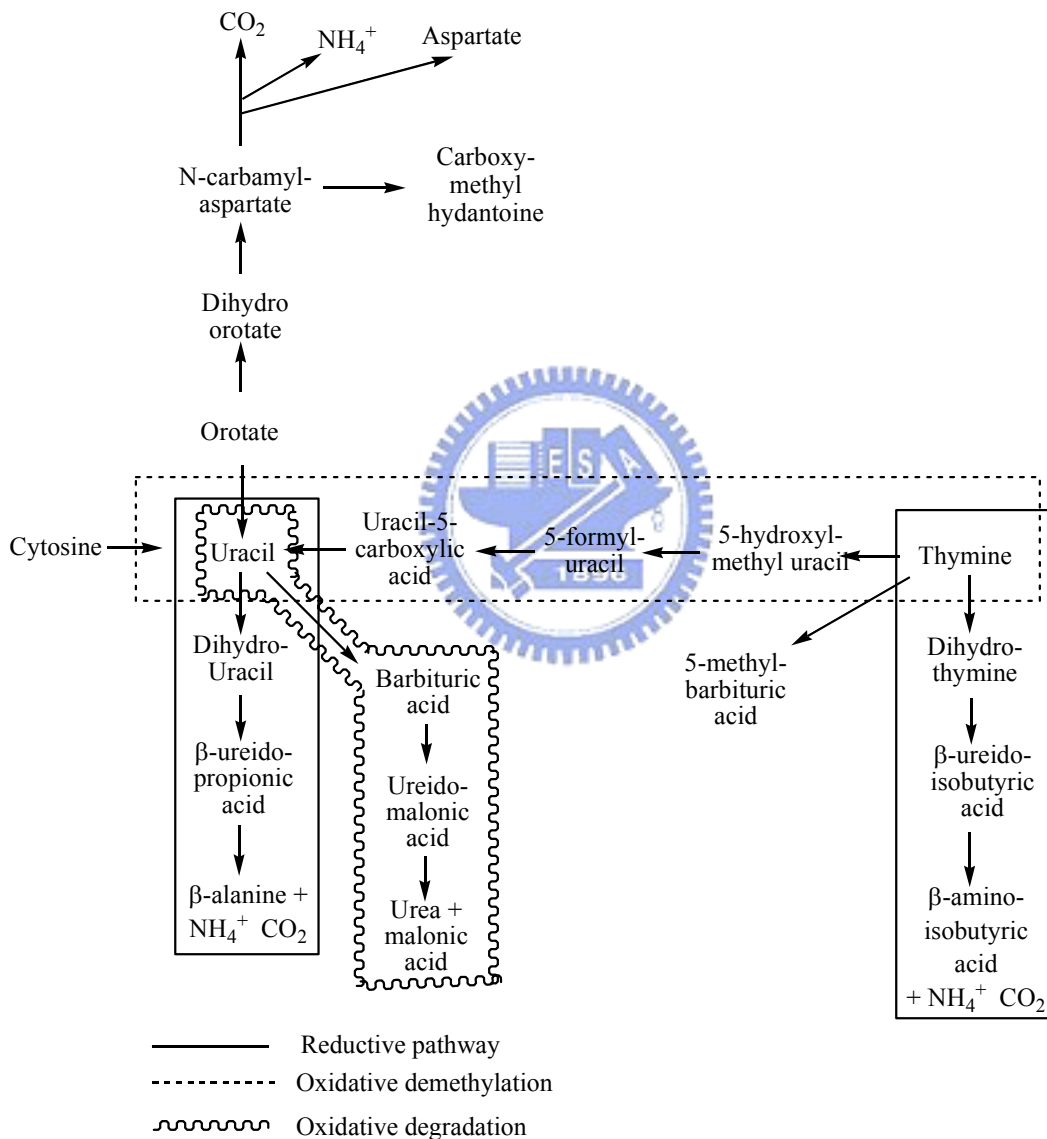


Figure 2. Pathways of pyrimidine degradation.

Among mechanisms of pyrimidine degradation (Figure 2), the reductive pathway was thought to be crucial in the nature (Wasternack, 1978; Vogels and van der Drift, 1976). The reductive pathway was also found in bacteria (Fink et al., 1954), yeast (LaRue and Spencer, 1968) and plants (Tsai and Axelrod, 1965). In reductive pyrimidine metabolism (Figure 3), uracil or thymine is first reduced to its dihydro-derivative by dihydropyrimidine dehydrogenase (also known as uracil dehydrogenase; EC 1.3.1.2) (Smith and Yamada, 1971).

Imidase (also identified as dihydropyrimidinase; EC 3.5.2.2) performs reversible hydrolytic ring-opening of dihydrouracil and dihydrothymine to *N*-carbamoyl- β -alanine and *N*-carbamoyl- β -aminoisobutyric acid, respectively. β -ureidopropionase (also called as β -alanine synthase or *N*-carbamoyl- β -alanine amidohydrolase; EC 3.5.1.6) catalyzes the irreversible hydrolysis of *N*-carbamoyl- β -alanine and *N*-carbamoyl- β -aminoisobutyric acid to β -alanine, β -aminoisobutyric acid, ammonia, carbon dioxide and β -amino acids (Sanno et al., 1970).

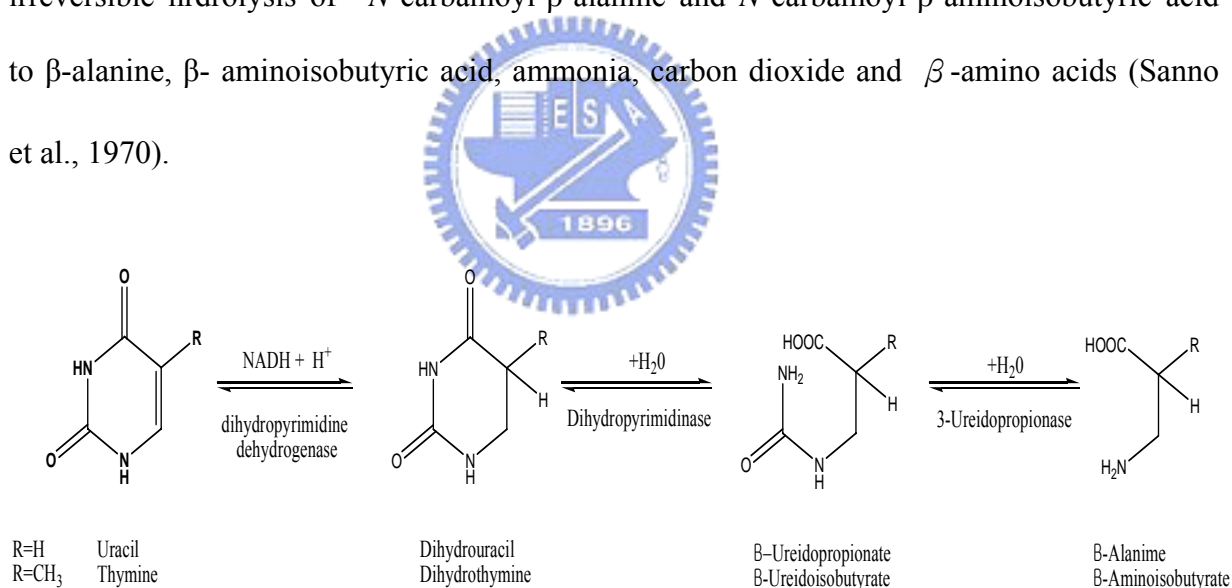


Figure 3. Reductive pathway of pyrimidine degradation.

The reductive pyrimidine degradation pathway is important especially in mammalian cells. In mammalian tissue, it is established that the degradation of uracil via dihydrouracil and *N*-carbamoyl- β -alanine is the only pathway leading to the biosynthesis of β -alanine (Wasternack et al., 1980), whereas in prokaryotic cells, β -alanine can be produced by α -

decarboxylation of aspartate (Williamson et al., 1979). In humans, the defect of enzymes involved in pyrimidine degradation leads to neurological disorders. The patients showed a variety of clinical phenotype including seizures or epileptic attacks, mental retardation, growth retardation and dysmorphic feature. In 1997, van Gennip et al. suggested that the clinical symptoms were related to the abnormal concentrations of the neurotransmitters β -alanine and β -aminoisobutyrate (van Gennip et al., 1997).

The physiological importance of imidase in the metabolism of humans was demonstrated by the following examples. Imidase was responsible for the catabolism of pyrimidine analogues that were used as pharmaceuticals for treatment of tumors, such as 5- fluorouracil, 5- bromouracil, 5- iodouracil and 5-nitrouracil (Naguib et al., 1985; Tuchman et al., 1988; Hull et al., 1988). It has been suggested that patients with a deficiency of imidase were at risk of developing severe 5-fluorouracil -associated toxicity, including death, after the administration of 5-fluorouracil (Hayashi et al., 1996; Sumi et al. 1998). Beside the pyrimidine analogues, imidase has been found to participate in the action of cardioprotective agent, dexrazoxane [ICRF-187; 1, 2-bis(3,5-dioxopiperazin-1-yl)propane]. Dexrazoxane was catalyzed ring opening to the active metal ion binding form by imidase (Hasinoff et al., 1994). The active form of dexrazoxane was able to quickly and completely chelate either free iron or displacing Fe^{3+} from its complex with doxorubicin and protect against the Fe^{3+} doxorubicin-induced inactivation of respiratory enzyme (Hasinoff, 1990).

In addition to drug metabolism, dihydropyrimidinase was highly active in all solid tumors, but not in their normal counterparts. Therefore it was suggested to serve as a good marker of tumorigenicity as well as a target for cancer chemotherapy of human solid tumors (Naguib et al., 1985).

1. 2 Industrial application of hydantoinase

D-hydantoinase is the microbial counterpart of imidase. In industry, *hydantoinase* were used for the production of optically pure D- and L- amino acids by resolution of racemic hydantoin derivatives (Syldatk et al., 1990; Syldatk et al., 1999; Olivieri et al., 1981; Ogawa and Shimizu, 1999) basis of the reactions shown in Figure 4.

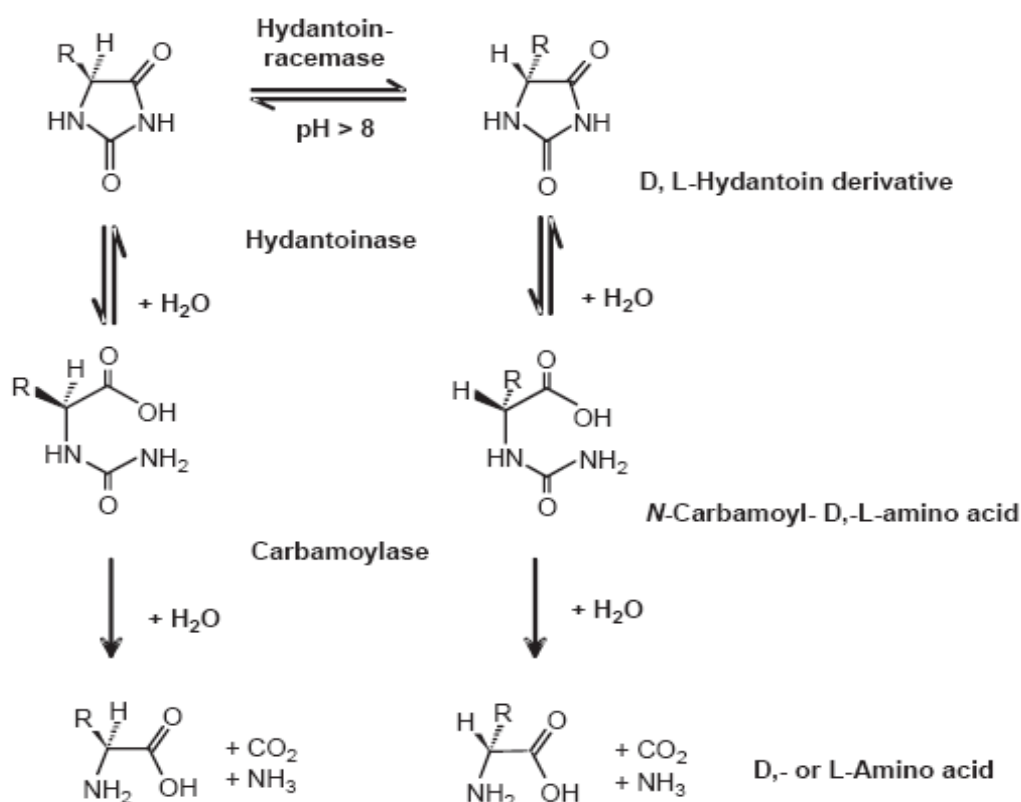


Figure 4. Production of D- and L- amino acids by imidase.

Chemical hydrolysis of hydantoin gives racemic amino acids, which requires resolution to optically pure amino acids. These products were various precursors for the synthesis of β -lactam antibiotics, peptide hormones, pyrethroids, and pesticides (Ogawa and Shimizu, 1999). The demand for these optical pure amino acids will increase, because several new drugs that are synthesized from them, are continuous to be product such as aspoxicillin and

cerbuperazone.

Among those amino acids, D-phenylglycine and D-*p*-hydroxyphenylglycine were used for the synthesis of semisynthetic penicillins and cephalosporins such as ampicillin and amoxicillin. Initially, the synthetic process for D-*p*-hydroxyphenylglycine involved two chemical steps and one enzymatic step (Takahashi et al., 1979). In figure 5, the substrate, DL-5-(*p*-hydroxyphenyl)hydantoin, is synthesized through an efficient chemical method involving the amidoalkylation reaction. Then, D-5-(*p*-hydroxyphenyl)hydantoin is hydrolyzed enzymatically to *N*-carbamoyl-D-*p*-hydroxyphenylglycine. Under pH 8 to 10, the L-isomer of the remaining 5-(*p*-hydroxyphenyl)hydantoin is racemized by base catalysis. Therefore, the racemic hydantoins were able to convert quantitatively into *N*-carbamoyl-D-*p*-hydroxyphenylglycine through this step.

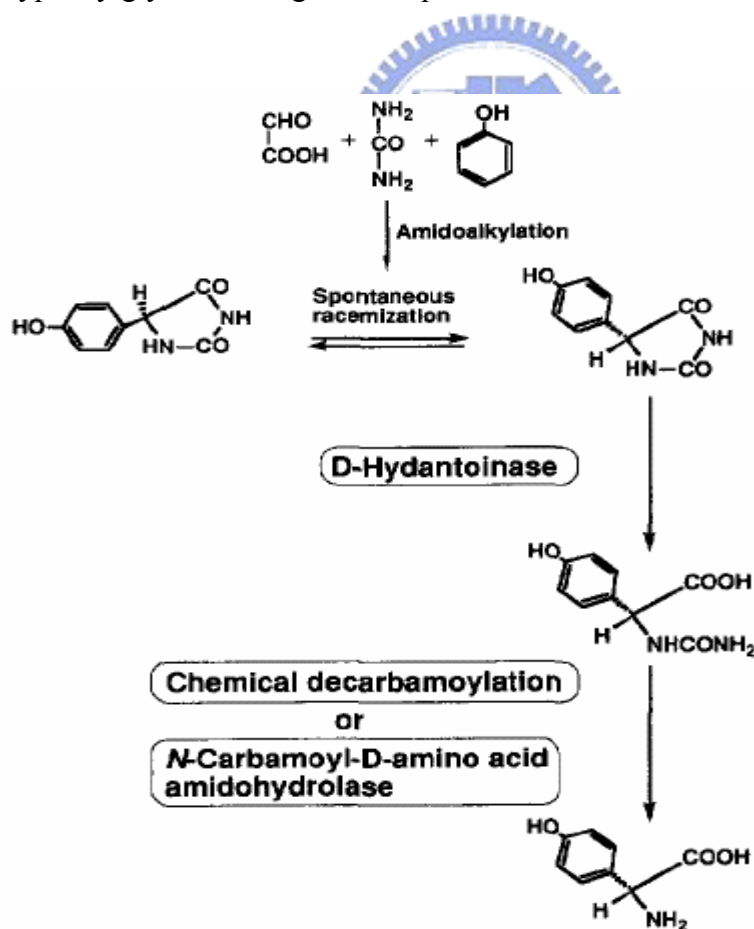


Figure 5. D-*p*-hydroxyphenylglycine production process.

Besides producing amino acid, other pharmaceutical compounds were also regioselectively produced by hydantoinase (Ogawa et al., 2000), such as 3-carbamoyl- α -picolinic acid. 3-carbamoyl- α -picolinic acid served as a versatile building block for the synthesis of pharmaceuticals and was considered to be a promising intermediate for the synthesis of modern agrochemicals such as nicotinoid insecticides (Kagabu et al., 1992; Moriya et al., 1993). The chemical synthesis of 3-carbamoyl- α -picolinic acid was prepared by alkaline hydrolysis of 2,3-pyridinedicarboximide, which was easily synthesized from 2,3-pyridinedicarboxylic acid and ammonia. But the hydrolysis occurred randomly at two amide bonds and resulted in the co-production of 2-carbamoyl- β -picolinic acid. Enzymatic regioselective hydrolysis of 2,3-pyridinedicarboximide (Figure 6) was an attractive method for overcoming this problem with 3-carbamoyl- α -picolinic acid synthesis. Those applications highlight the importance of hydantoinase investigation.

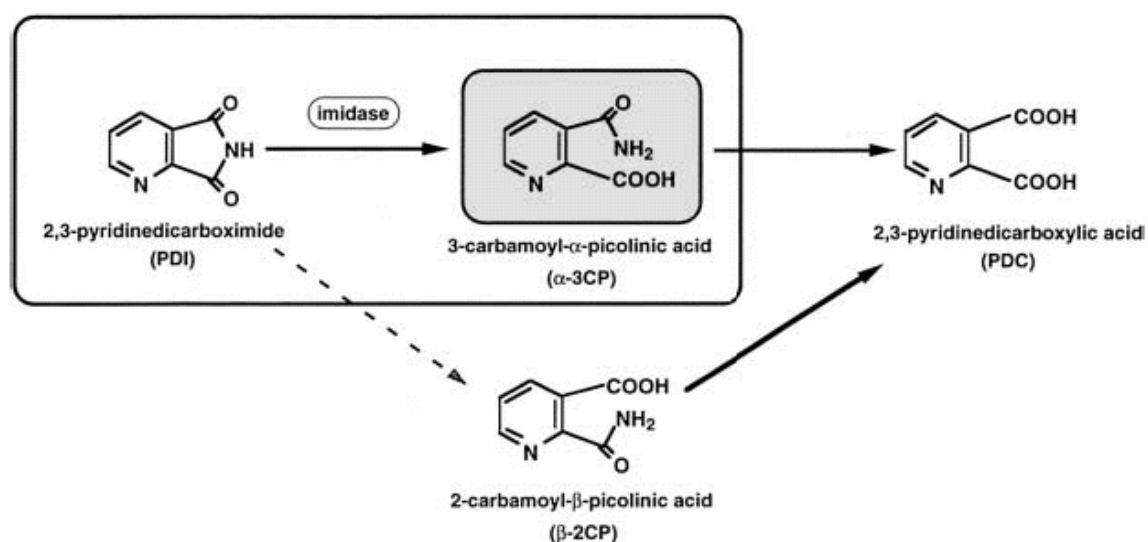


Figure 6. Hydrolysis of 2,3-pyridinedicarboximide to 3-carbamoyl- α -picolinic acid.

1.3 Properties of imidase

Wallach and Grisolia (1957) demonstrated that 80% purified enzyme from calf liver

hydrolyzed hydantoin as well as dihydrouracil and dihydrothymine. Therefore, they assumed that dihydropyrimidinasases were identical to the hydantoinases discovered earlier. However, with increased knowledge of imide-hydrolysis enzymes, significant variations were found in sequence, subunit composition, substrate specificity, metal content and other requirements for enzymes catalyzed with similar reactions from different organisms (Syldatk et al., 1999). Dihydropyrimidinasases purified from bovine (Brooks et al. 1979, 1983) and rat livers (Kikugawa et al., 1994) were homotetrameric enzymes with native molecular masses of 226 kDa and 215 kDa respectively. The subunit composition and molecular masses corresponded to those dihydropyrimidinasases from bacteria (Takahashi et al., 1978; Morin et al., 1986). However, the dihydropyrimidinasase from *Bacillus stearothermophilus* SD-1 (Lee et al., 1997) and *Pseudomonas stutzeri* (Xu and West, 1994) differed with respect to subunit composition. Both enzymes were homodimers with native molecular masses of 102 kDa and 115 kDa respectively. Currently, crystal structures of hydantoinase from *Thermus* sp. (Abendroth et al., 2002a), *Bacillus stearothermophilus* (Cheon et al., 2002), *Arthobacter aurescens* (Abendroth et al., 2002b), *Burkholderia pickettii* (Xu et al., 2003) and *Bacillus* sp. (Radha Kishan et al., 2005) were available. According to those structures, hydantoinases belonged to the urease family and contained a catalytic TIM-barrel domain where the active sites were present on the C-terminal end of the β -strands. Beside TIM-barrel, hydantoinases contained a second domain formed from the N-terminal and C-terminal amino acid residues of the polypeptide chain. This domain was rich in β -strands and believed to be involved in multimer formation (Kim and Kim, 1998).

Hydantoinases from most species were reported to be thermostable (Table 1). The structural comparison of hydantoinase has been revealed insight into the molecular basis of the differential thermostability of D-hydantoinases. The more thermostable *Thermus* sp. hydantoinase contained more aromatic residues in the interior of the structure than

hydantoinase from *Bacillus stearothermophilus* and *Burkholderia pickettii* (Xu et al., 2003). Hydantoinase from *Thermus* sp. had more salt bridges and hydrogen-bonding interactions and less oxidation susceptible Met and Cys residues on the protein surface than from *Bacillus stearothermophilus* and *Burkholderia pickettii*. Besides, *Thermus* sp. hydantoinase also contained more rigid Pro residues. Although most hydantoinases were thermophile, hydantoinase purified from *Oreochromis niloticus* fish was mesophile (Huang and Yang, 2003). Analysis of the circular dichroism spectra from fish liver, pig liver, and bacterial hydantoinase showed a different secondary structure. Mesophile fish hydantoinase gave the weakest signal in the far-UV region, which corresponded to an apparent lower fraction of secondary structures, as compared to those of thermophilic hydantoinase. The less organization of fish hydantoinase might cause its possibly higher flexibility and also lead to its instability. All these factors were likely to make major contributions to the varying thermostability of these enzymes.

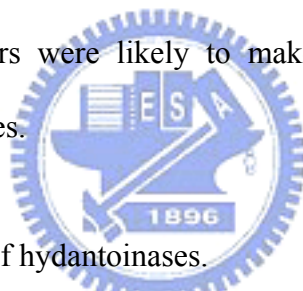


Table 1. Subunit and stability of hydantoinases.

Example for diversity of hydantoinase			
Subunit	Bovine, rat liver	tetramer	Brooks et al., 1983, <i>Arch. Biochem. Biophys.</i> , 226, 469 Kikugawa et al., 1994, <i>Eur. J. Biochem.</i> , 219, 393
	<i>Agrobacter crystallopoietes</i> <i>Thermus</i> sp.	tetramer	Siemann et al., 1999, <i>J. Mol. Catal. B</i> , 6, 387 Abendroth et al., 2002, <i>JMB</i> , 320, 143
	<i>Bacillus stearothermophilus</i> SD1, <i>Pseudomonas stutzeri</i>	dimer	Lee et al., 1997, <i>Appl. Biochem. Biotechnol.</i> , 62, 251 Xu and West, 1994, <i>Arch. Microbiol.</i> , 161, 70
stability	Fish liver	psychrophiles	Huang and Yang, 2003, <i>BBRC</i> , 312, 467
	Pig liver <i>Burkholderia pickettii</i>	mesophile	Su and Yang, 2000, <i>PEP</i> , 19, 289 Xu et al., 2003, <i>J. Bacteriol.</i> , 185, 14

Generally, hydantoinases are able to hydrolyze dihydrouracil, dihydrothymine, hydantoin, and 5'-monosubstituted hydantoin. However, the substrate specificities for different species hydantoinase were very different. Campbell (1958) purified an enzyme from *Clostridium*

uracilum that only hydrolyzed dihydrouracil but not dihydrothymine or hydantoin. Runser and Meyer (1993) isolated an enzyme from *Agrobacterium sp.* that hydrolyzed hydantoin and 5'-monosubstituted hydantoin derivatives but no dihydropyrimidines. Furthermore, Ogawa et al. (1995, 1997) reported hydantoinase from *Blastobacter sp.* that hydrolyzed dihydropyrimidines and hydantoin but had a different metabolic function from dihydropyrimidinases.

Table 2 is the substrate specificity of hydantoinases from different bacteria. Hydantoinase from *Pseudomonas striata* was more like to use dihydrouracil as substrate than hydantoin, but in *Agrobacterium sp.* IP I-671 there is no activity of dihydrouracil. The hydantoinase from *Bacillus stearothermophilus* SD1 preferred nonsubstituted hydantoin as substrate (Lee et al., 1997). Another hydantoinase from *Bacillus thermocatenulatus* GH2 used both aromatic hydantoin derivatives and nonsubstituted hydantoin as substrates (Park et al., 1999). Meanwhile, their sequences were as much as 92% homologous with each other. Although the overall structure of hydantoinase and the structure of the catalytic active site were strikingly similar, the amino acids that composed the substrate-binding site were less conserved and had different properties, which might dictate the substrate specificity.

Table 2. substrate specificity of different hydantoinases.

Substrate	Activity %					
	<i>Pseudomonas striata</i>	<i>Agrobacterium sp.</i> IP I-671	<i>Bacillus stearothermophilus</i> SD-1	<i>Bacillus stearothermophilus</i> GH2	<i>Blastobacter sp.</i> A17p-4	<i>Escherichia coli.</i> K-12
Dihydrouracil	769	0	46	27	245	N.R
Hydantoin	100	100	100	100	100	100
5'-Isopropylhydantoin	115	1470	5	11	N.R.	230
5'-Phenylhydantoin	192	N.R	42	234	32	792
5'- <i>p</i> -Hydroxyphenylhydantoin	123	640	17	90	8	889
Reference	Takahashi et al., 1978	Runser and Meyer, 1993	Lee et al., 1995	Park et al., 1999	Soong et al., 1999	Kim et al., 2000

N.R. : No reported in reference

Cyclic amidohydrolases (EC 3.5.2.–), include hydantoinase, dihydropyrimidinase, allantoinase and dihydroorotase, are functionally and structurally related superfamily enzymes. All of those were metalloproteins that evolved from a common ancestor. Table 3 shows the metal content in hydantoinases from different species. Before the resolution of crystal structure of *Bacillus stearothermophilus* SD-1 hydantoinase, the enzyme was reported bound 1 mol Mn²⁺/mol subunit (Lee et al., 1997). The authors reported that this enzyme was preincubated with manganese for 2 days and that only manganese and no other metal was analyzed. It was possible that incubation with manganese led to an exchange of a previously bound metal (e.g. Zn²⁺). Furthermore, manganese might bind non-specifically to the enzyme in addition to other metal ions, which would not have been detected because the enzyme was only analyzed for manganese. Therefore it was not clear whether the naturally bound metal ion of this enzyme was actually manganese. Recently, the crystal structure of *Bacillus stearothermophilus* SD-1 hydantoinase had been resolved and suggested it contain di-zinc per subunit (Cheon et al., 2002). In conclusion, hydantoinase purified from animal and bacteria were reported to contain one and two metal ions per subunit respectively.

Table 3. Metal content of hydantoinase.

	Source	metal per subunit	Method	
Metal	Bovine liver	one zinc	AAS	Brooks et al., 1983, <i>Arch. Biochem. Biophys.</i> , 226,469
	Rat liver		AAS	Kikugawa et al., 1994, <i>Eur. J. Biochem.</i> , 219,393
	Pig liver		ICP-MS	Su and Yang, 2000, <i>PEP</i> , 19, 289
	Fish liver		ICP-MS	Huang and Yang, 2003, <i>BBRC</i> , 312, 467
	<i>Arthrobacter aureescens</i>	two zinc	ICP-AES	May et al., 1998, <i>J. Mol. Catal. B</i> , 5, 367
	<i>Bacillus stearothermophilus</i>	two zinc	ICP-AES	Cheon et al., 2002, <i>Biochemistry</i> , 41, 9410
	<i>Thermus</i> sp.	two zinc	Crystal structure	Abendroth et al., 2002, <i>JMB</i> , 320, 143
	<i>Bacillus</i> sp. AR9	two manganese	Crystal structure	Radha Kishan et al., 2005, <i>JMB</i> , 347,95

Crystal structures of hydantoinase from *Thermus* sp. (Abendroth et al., 2002), *Bacillus stearothermophilus* (Cheon et al., 2002), *Arthrobacter aureescens* (Abendroth et al., 2002b)

Burkholderia pickettii (Gerlt et al., 2003) and *Bacillus* sp. AR9 (Radha Kishan et al., 2005) are available. They all consists a core TIM-barrel fold (Gerlt and Raushel, 2003) and the metal binding residues were highly conserved. In the crystal structures of bacterial hydantoinases, six metal binding residues (four histidines, one carboxylated lysine and one aspartic acid) were coordinated with two metal ions and stabilized the orientation of binuclear center (Figure 7). On the other hand, the enzyme purified from mammalian and fish contained about 1 mol Zn^{2+} /mol subunit, but the enzyme from bacteria contained 2 mol metal ion / mol subunit.

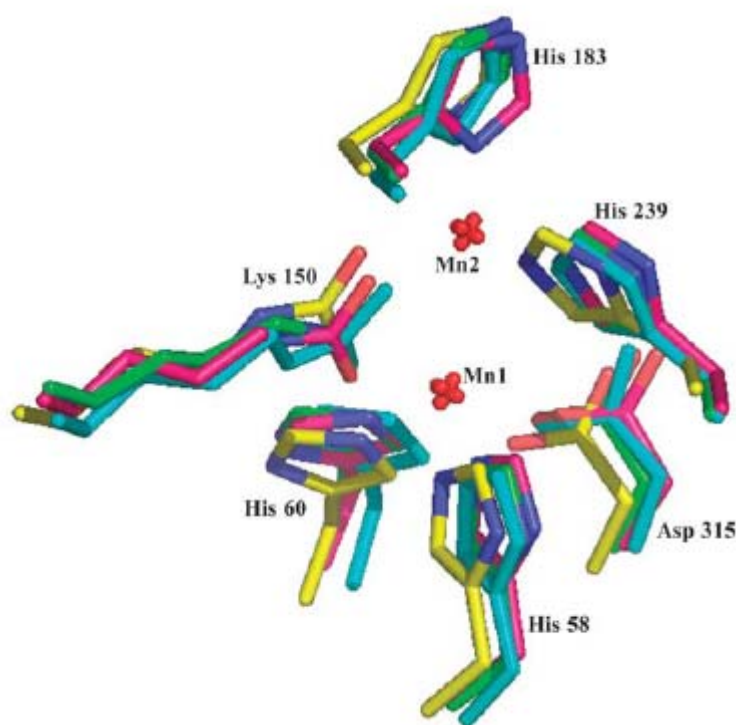


Figure 7. The conserved metal binding residues in the active site from different hydantoinase.

It has been proposed previously that the removal of the imide proton forces the C4–N3–C2–N1 toward greater planarity in accommodating the delocalized electrons, which is the driving force for imide hydrolysis catalyzed by imidase. The function of the metal ion in imidase is to coordinate substrate and maintain a suitable active site environment but not

directly involve the ionization of a water molecule. Instead, a histidine may be responsible for the ionization of water because pK_{a1} at around 6–6.3 are observed through the pH profiles of native and metal reconstituted imidasases. Conserved aspartic acid is also found to be important for imide hydrolysis and may function as a proton donor/acceptor. Aspartic acid may be needed for the dehydration of N-carbamoyl acid (reverse reaction of the hydrolysis of dihydrouracil), which is catalyzed by imidase under acidic conditions. The metal coordinated water may be activated by ionization, polarization, or poised for displacement. Imidase metal ion may function as a Lewis acid for catalysis to stabilize the developing negative charge of imide in the transition state or to fix the orientation of the metalbound substrate so that it is in position for nucleophilic attack by water or a hydroxide ion activated by a histidine.

In the bacterial imidase, allantoinase and dihydroorotase, the two divalent metal ions are presented. The carboxylated lysine residue bridges the two metal ions. However, with mammalian imidase and the fish imidase, the protein apparently functions with single divalent metal ions in the active site. Surprisingly, *Aquifex aeolicus* dihydroorotase has been reported that also has single divalent metal ions in the active site recently (Philip D et al., 2005). The structure of *Aquifex aeolicus* dihydroorotase has one zinc atom in the active site bounded by His61, His63, Asp153, and HOH1. In figure 8, the superposed zinc ligands are shown for *Aquifex aeolicus* dihydroorotase (grey), *E. coli* dihydroorotase (blue) and *Thermus* sp. hydantoinase (green). This metal site corresponds to the alpha zinc site in *E. coli* dihydroorotase and *Thermus* sp. hydantoinase.

The reason for different numbers of coordinated metals is mystery and the mechanism for metal-playing enzyme-hydrolyzing is poorly understood. Therefore, we would clone the fish liver imidase and then use Homology Modeling, Molecular Docking and biological techniques to study the differences between various imidasases.

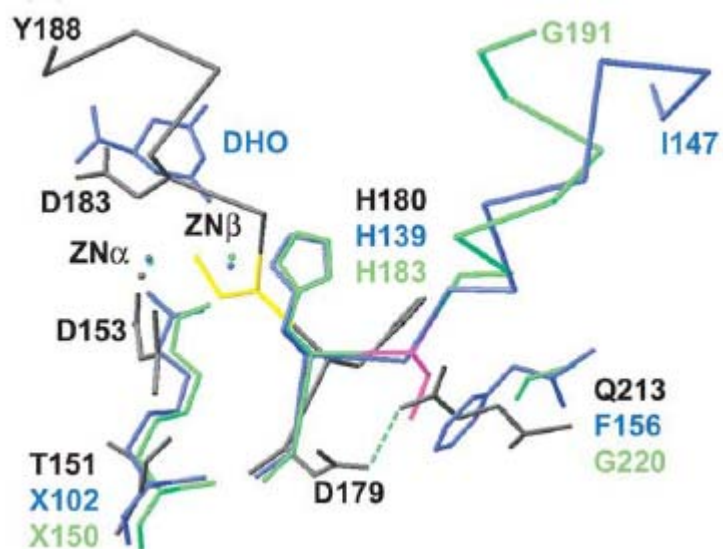


Figure 8. The superposed metal binding ligands in the active site.

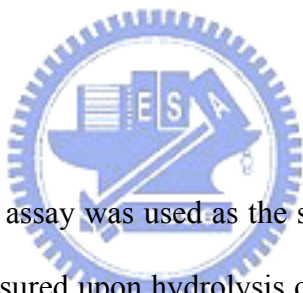


2. Experimental procedures

2.1 Materials

The resistance of water used was more than 18 M-ohms, which was purified by reverse osmosis followed by passage through a Millipore Reagent Water System (Millipore, Bedford, MA, USA). Octyl Sepharose CL-4B, chelating Sephacel (fast flow), and HiTrap Q columns were purchased from Amersham Biosciences (Taiwan Branch). Bis-Tris propane, PMSF, 5-hydantoinacetic acid, parabanic acid, phthalimide and 3-iminoisoindoline were purchased from Sigma (U.S.A.). EDTA, Tris-HCl, potassium phosphate, sodium chloride, sodium hydroxide, and zinc acetate were obtained from J.T. Baker (U.S.A.). Hydroxyapatite Sephacel was purchased from Biosepra (U.S.A.). Trypsin was purchased from Promega (U.S.A.). All other chemicals were obtained commercially at the highest purity possible.

2.2 Enzyme Standard Assay



A rapid spectrophotometric assay was used as the standard assay. Briefly, the decrease in absorbance at 298 nm was measured upon hydrolysis of phthalimide as the substrate at 25°C. To start the reaction, the enzyme solution was added into a 1 ml solution, containing 1 mM phthalimide and 100 mM Bis-Tris propane at pH 7.0. Under these conditions, a change in A_{298} of 2.26 represents the hydrolysis of 1 mol of the substrate. The hydrolysis of the substrate was monitored with a UV/Vis spectrophotometer (Hitachi U 3300).

2.3 Protein concentration

The protein concentration of enzyme solution was determined by A_{280} or BCA protein assay (Sigma, USA) using bovine serum albumin as a standard. For the homogeneous imidase, 1U of A_{280} equals 1.17 mg/ml imidase based on the BCA protein assay. Similar results were determined for all the three enzymes studied in this report.

2.4 Protein purification

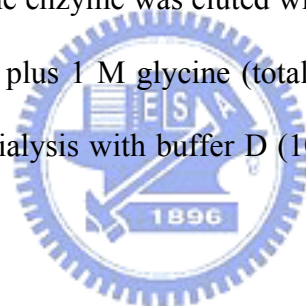
Imidase taken from pig liver and hydantoinase (bacterial counterpart of imidase) taken from *Agrobacterium radiobacter* were purified according to the published procedures. Fish liver imidase was purified as described below. Fish (*Oreochromis niloticus*) were purchased from traditional market. All procedures for protein purification were conducted at 4°C or in an ice bath. The pH of buffers for enzyme purification refers to the measurements taken at room temperature. An FPLC system (Pharmacia) and a Pharmacia column were used for column chromatography.

Step 1: extract. The imidase was extracted from fresh fish liver (*Oreochromis niloticus*) (about 200 g) with a 400 ml buffer A (50 mM potassium phosphate, 1 mM PMSF, and 2mM EDTA at pH 8). A fair amount of lipid-like substance was found in the fish liver during the enzyme extraction and removed by filter papers (Whatman, No.1). The suspension was centrifuged at 20,000×g for 1 hr to remove precipitates.

Step 2: salting out. Ammonium sulfate (equivalent to 35% of saturation) was slowly added to the enzyme extract and stirred for 60 min. The suspension was centrifuged at 20,000 ×g for 30 min to remove precipitate and an additional ammonium sulfate was added into a supernatant fluid to 60% saturation. After gentle stirring for 60 min, the resultant precipitate was collected by centrifugation (20,000×g, 30min). The precipitate was dissolved in buffer B (10 mM potassium phosphate, 1.5 M ammonium sulfate, 1 mM PMSF, and 2 mM EDTA at pH 7). Then it was stirred gently for 120 min. Insoluble substances were removed by centrifugation (20,000×g, 30 min). The dissolution of the enzyme precipitate was repeated once to ensure that all the imidase activity was collected in the solution.

Step 3: octyl Sepharose. The enzyme solution was applied to a column (4.4×10 cm) of octyl Sepharose CL-4B that had been equilibrated with buffer B followed by washing with 400 ml of the same buffer. The protein was eluted with a reverse linear salt gradient of 1.5–0 M ammonium sulfate using 320 ml each of buffer B and buffer B minus ammonium sulfate. Active fractions were pooled and desalted by dialysis with buffer C (20 mM potassium phosphate, 1 mM PMSF, and 0.5 M NaCl at pH 7) .

Step 4: chelating Sephacel. The enzyme solution in buffer C was applied to a column (1.6 ×10 cm) of chelating Sephacel (fast flow) that had been treated with 1 gel volume of 0.2 M zinc acetate. The column was then equilibrated with buffer C. The loaded column was washed with 150 ml of buffer C, and the enzyme was eluted with a linear glycine gradient from 0 to 1 M with buffer C and buffer C plus 1 M glycine (total volume 240 ml). The active fractions were pooled and desalted by dialysis with buffer D (10 mM potassium phosphate and 1 mM PMSF at pH 7) .



Step 5: hydroxyapatite Sephacel. The imidase solution was loaded into a column (1.6×10 cm) of hydroxyapatite Sephacel that had been equilibrated with buffer D. Imidase was eluted with a linear potassium phosphate gradient from 0.02 to 0.4 M (total in a volume of 300 ml, including 1 mM PMSF at pH 7).

Step 6: Hitrap Q Sepharose. The desalted enzyme solution was loaded into a Hitrap Q column (5 ml, previously equilibrated with buffer D). The enzyme was eluted by buffer D (total volume 25 ml) without a salt gradient. Homogeneous imidase was obtained from active fractions. By the standard assay, the specific activity of fish imidase was 86 μ mol/min/mg in a typical experiment.

2.5 *In gel digestion and identification using LC-ESI-MS*

The spots of interest were excised and digested in gel with trypsin according to Shevchenko's method (Shevchenko et al., 1996). The digestion sample was taken up and analyzed using LC-ESI-MS. The results were correlated with the sequence database using the NCBI and SwissProt database and analyzed by Mascot software.

2.6 *RNA extraction and cDNA synthesis*

The fish (*Tetraodon nigroviridis*) were purchased from a pet shop. Fish liver were dissected out and total RNA was extracted with RNeasy® Protect Mini Kit (Qiagen, U.S.A.) following the manufacturer's protocol and cDNA synthesis was carried out using SuperScript III First-Strand Synthesis System for RT-PCR Kit (Invitrogen, U.S.A.).

2.7 *PCR cloning and sequencing*

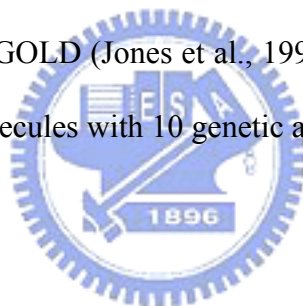
The synthesized cDNA was used as a template for PCR to clone the imidase from fish (*Tetraodon nigroviridis*). The forward primer was 5'-atggcagaagccggcgagatc-3', and reverse primer was 5'-tcagtcagacgttcccagagcaac-3'. The amplification conditions were 30 cycles of 95 °C for 30 sec, 55 °C for 1 min and 72 °C for 2 min. The PCR product was cloned into pGEM-T easy vector (Promega, U.S.A.) and transformed into DH5 α . Plasmid DNA was extracted by alkaline lysis (Premier, Taiwan). The cDNA clone was subjected to sequencing reaction with T7 and SP6 primers and sequenced on an automated DNA sequencer.

2.8 *Sequence analysis*

The sequence was compared with those in the database using the BlastN algorithm. Protein sequence alignment and percentage identities were calculated using MuliAlin and ClustalW software.

2.9 Homology Modeling and Molecular Docking

The pair-wise alignment of *Agrobacterium radiobacter* (Chao et al., 2000) and *Burkholderia pickettii* hydantoinase sequences are made by ClustalW and revealed a 92.6% sequence identity. The 3D-structure of *Agrobacterium radiobacter* hydantoinase was modeled by automatic modeling at the Swiss-Model server (Schwede et al., 2003; Guex and Peitsch, 1997), which the X-ray crystal structure of *Burkholderia pickettii* hydantoinase (1NFG) was selected as template. A carboxylated lysine was observed in 1NFG, where the modified lysine was conserved in amidohydrolase superfamily. The post modified lysine was manually altered a carboxyl group. Then two zinc ions were added into model structure according to resolved X-ray structure. Fish liver imidase were modeled by automatic modeling at the Swiss-Model server, the X-ray crystal structure of *Bacillus Sp.* (1YNY) was selected as template. These two model structures were used in GOLD (Jones et al., 1997) as templates to dock parabanic acid and 5-hydantoinacetic acid molecules with 10 genetic algorithm runs.



2.10 Inhibition assay

Non-substrate compounds were examined experimentally as potential inhibitors of imidase. The inhibition assay was done in a similar standard assay condition using 3-iminoisoindoline or phthalimide as substrate. After the inhibitor was mixed with assay solution, the enzyme was added to start the measurement.

2.11 Analysis of Kinetics Data

Results of kinetics experiments were analyzed using nonlinear or linear regression to fit the appropriate equation to the data. The rate constants (K_m , V_{max} and K_i) were obtained using SigmaPlot 2001, V7.0 and Enzyme Kinetics Module, V1.1 (SPSS Inc., Chicago, IL). Data used represent mean values derived from three determinations.

3 Results and discussion

3.1 Purification of fish liver imidase

Imidase from fish liver (*Oreochromis niloticus*) was purified about 2630-fold with a 9% yield (Table 1). A homogeneous protein was obtained as determined by SDS-PAGE (Figure 1). The molecular weight of a single polypeptide chain was estimated to be around 56,000.

3.2 Identification of fish liver imidase

Through in-gel digestion and identification using LC-ESI-MS (Figure 2), several peptide fragments were matched with. As showed in figure 3, the amino acid coverage of human dihydropyrimidinase is 8% and the matched peptide fragments were “-MFMAYK-, -ALGKDDFTK-, -IPNGVNGVEDR-, -MSVIWEK-, -GVHSGKMDENR-”. The amino acid coverage of putative *Canis familiaris* dihydropyrimidinase is 12% and the matched peptide fragments were “-MFMAYK-, -EIGAIALVHAENGDLIAEGAK-, -ALGKDDFTK-, -IPNGVNGVER-, -MSVIWEK-, -GVHSGKMDENR-”. The amino acid coverage of mouse dihydropyrimidinase related protein-5 is 4% and the matched peptide fragments were “-MSVVWER-, -MDENRFVAVTSSNAAK-, -FVAVTSSNAAK-”. Besides, the results were correlated with the sequence database by Mascot software indicated two unnamed proteins, *Tetraodon nigroviridis* unnamed protein (CAF98068) and *Xenopus laevis* unnamed protein (gi|54311199), have high amino acid coverage (19% and 11% respectively). Amino acid alignment revealed 73% homology with *Homo sapiens* dihydropyrimidinase and *Tetraodon nigroviridis* unnamed protein has the six conserved amino acids in the active site. The condition is the same in the *Xenopus laevis* unnamed protein (sequence identity is 78%). The detection results of LC-ESI-MS were demonstrated that the purified enzyme is imidase.

3.3 Cloning of fish liver imidase

Total RNA was extracted from *Tetraodon nigroviridis* liver and cDNA was synthesized by RT with oligo d(T) primer. Base of sequence (CAF98068), a pair of primers, fDHP N-ter (5'-atggcagaagccggcgagatc-3') and fDHP C-ter (5'-tcagtcagacgttcccagagcaac-3'), were designed. After PCR, the full-length cDNA of imidase was obtained. The nucleotide sequence and the deduced amino acid sequence are shown in figure 4. The complete nucleotides of fish imidase contained a 1503 bp open reading frame (ORF) and encoded 500 amino acids. The deduced amino acid sequence of *Tetraodon nigroviridis* imidase shared relatively high identities with *Homo sapiens* imidase (NP_001376) and *Rattus norvegicus* imidase (Q63150).

3.4 Homology Modeling and Generation of the active site structure

Currently, crystal structures of hydantoinase from *Thermus* sp. (Abendroth et al., 2002), *Bacillus stearothermophilus* (Cheon et al., 2002), *Burkholderia pickettii* (Gerlt et al., 2003) and *Bacillus* sp. AR9 (Radha Kishan et al., 2005) are available. They all consist of a core (β/α)₈-barrel fold (Gerlt and Raushel, 2003). A similar fold was also reported in the α -subunits of urease from *Klebsiella aerogenes* and *Bacillus pasteurii*, dihydroorotase from *E. coli*, and the phosphotriesterase from *Pseudomonas diminuta* (Jabri et al., 1995; Benini et al., 1999; Thoden et al., 2001; Vanhooke et al., 1996). In all those structures, six highly conserved metal binding residues, four histidines, one carboxylated lysine, and one aspartic acid were coordinated with two metal ions to stabilize the orientation of the binuclear center. According to the crystallized structures with bound inhibitors in urease, dihydroorotase, and phosphotriesterase, the active site of hydantoinase could be expected to locate in this region. In hydantoinase, allantoinase and dihydroorotase, the two divalent metal ions are presented. The carboxylated lysine residue bridges the two metal ions. However, in mammalian

imidase and fish liver imidase, they function with single divalent metal ion in the active site. The mystery about the different number of metals in the different species has been unclear all the time. Surprisingly, *Aquifex aeolicus* dihydroorotase has recently been reported that also has single divalent metal ions in the active site, and the metal site was correlated to the α -zinc site in *E. coli* dihydroorotase and bacterial hydantoinase.

To build up the active site of hydantoinase from *Agrobacterium tumefaciens* and fish liver imidase from *Tetraodon nigroviridis* performed in this study, the crystal structure of *Burkholderia pickettii* hydantoinase (PDB code 1NFG.) and Bacillus sp. AR 9 (PDB code 1YNY) were used as template respectively. The sequence identity of the *Agrobacterium tumefaciens* hydantoinase and *Burkholderia pickettii* hydantoinase is 92.6% (Figure 5). In the structure of *Agrobacterium tumefaciens* hydantoinase (Figure 7b), the active site that contains binuclear centre is located at one end of the TIM barrel distant from the β -rich domain at the end of a roughly 15 Å deep hydrophobic cleft. The metal binding residues are H57, H59, Kcx148, H181, H237, and D313. α -zinc is coordinated by H57 N ϵ 2, H59 N ϵ 2, Kcx148 O \times 2 and D313 O δ 1. β -zinc is coordinated by Kcx148 O \times 1, H181 N δ 1, and H237 N ϵ 2.

The active site of *Tetraodon nigroviridis* imidase was modeled used Bacillus sp. AR 9 (PDB code 1YNY) as template. The sequence identity of the *Tetraodon nigroviridis* imidase and Bacillus sp. hydantoinase is 42% (Figure 6). In previous study, biochemical analysis of mammalian and fish (*Oreochromis niloticus*) liver imidase found one tightly bound zinc atom per molecule but its specific binding site, α or β , was unknown. D321, a conserved catalytic residue, is 2.45 Å from Zn $^{\alpha}$ and 4.77 Å from Zn $^{\beta}$ in model structure. *Aquifex aeolicus* dihydroorotase structure has only one metal ion in α - site. So one zinc ion was added into modeled structure in the α - site coordinated by H62 N ϵ 2, H64 N ϵ 2, D321 O δ 1 and HOH1. Comparing structures of *Tetraodon nigroviridis* imidase with *Agrobacterium tumefaciens* hydantoinase, the side chain of K154 without post modification in fish imidase was shorter

than Kcx148 in hydantoinase. K154 in fish imidase swings out the active site (Figure 7a) and away from α - zinc.

3.5 Molecular Docking

In our previous study, molecular docking selected two compounds, 5-hydantoinacetic acid and parabanic acid, can enter the active site of *Agrobacterium tumefaciens* hydantoinase and have a reasonable orientation for reaction. Due to the metal contents in the various species were different, we furthermore docked 5-hydantoinacetic acid (Figure 8) and parabanic acid (Figure 9) into *Tetraodon nigroviridis* imidase by GOLD. Interestingly, both of them have different orientations than in *Agrobacterium tumefaciens* hydantoinase.

Computational results were confirmed by a series enzymatic assays. The substrate activities were measured at 25°C in 100 mM Bis-Tris propane at pH 7 and using parabanic acid or 5-hydantoinacetic acid as substrate. Substrate activity results (Table 2) showed that *Agrobacterium tumefaciens* hydantoinase did hydrolyze the 5-hydantoinacetic acid and parabanic acid but non determined in *Oreochromis niloticus* imidase. Moreover, inhibition assay (Table 3) showed 5-hydantoinacetic acid and parabanic acid were not substrates in *Oreochromis niloticus* fish imidase, but competitive inhibitors. Pig liver imidase with one tightly bound zinc atom per molecule also had identical behavior with *Oreochromis niloticus* imidase.

A reasonable explanation is that the open location and free H181 and H237 in *Tetraodon nigroviridis* imidase will form different active site with *Agrobacterium tumefaciens* hydantoinase. Molecular docking of 5-hydantoinacetic acid into *Agrobacterium tumefaciens* hydantoinase showed it can enter the active site, and N2 of 5-hydantoinacetic acid lay within hydrogen bonding distance of the carbonyl oxygen of T286 (2.73 Å), O3 form a hydrogen bond with peptic NH of T286 (2.86 Å) and peptic NH of N335 had a distance of 3.43 Å with

O4 of the 5-hydantoinacetic acid. However in *Tetraodon nigroviridis* imidase structure, the β -zinc site is open and GOLD docking result showed that 5-hydantoinacetic acid can enter the active site, but the imide ring was swung out and away from the metal. For *Tetraodon nigroviridis* imidase, 5-hydantoinacetic acid is not the substrate, but a competitive inhibitor.

GOLD docking of parabanic acid into *Agrobacterium tumefaciens* hydantoinase also showed it can enter the active site, with N2 of parabanic acid hydrogen bonding with carbonyl oxygen of T286 (2.91 Å), O3 forming a hydrogen bond with peptic NH of T286 (2.86 Å) and peptic NH of N335 had a distance of 3.35 Å with O4 of the parabanic acid. GOLD docking with parabanic acid into *Tetraodon nigroviridis* imidase showed it tended to the open location and H181 and H237 equal to the β -zinc ligands in hydantoinase can interact with parabanic acid by forming hydrogen bond. Peptic NH of H187 had a distance of 3.45 Å with O3 of the parabanic acid, O1 form a hydrogen bond with peptic NH of H243 (4.25 Å) and peptic NH of K154 had a distance of 3.01 Å with O5 of the parabanic acid. Parabanic acid can enter the active site and form weak hydrogen bonds; maybe this is the reason parabanic acid is not a strong competitive inhibitor for *Tetraodon nigroviridis* imidase.

3.6 Proposed catalytic mechanism of fish liver imidase

Fish liver imidase would contain a mononuclear metal center within the active site. It is proposed that metal ion in imidase is to coordinate substrate and maintain a suitable active site. The α -zinc ion is bound by His62, His64, Asp321 and HOH. Nucleophilic attack by the hydroxide is assisted by general base catalysis from the side chain carboxylate of Asp321. Then the intermediate is stabilized by ligating to metal ion. Collapse of this intermediate and cleavage of the carbon-nitrogen bond are assisted by the simultaneous protonation of the amide nitrogen by Asp321. The metal ion stabilized the developing negative charge of imide substrates.

4. Conclusions

The mystery about the different number of metals in the different species has been unclear all the time. In this study, the sequence of *Tetraodon nigroviridis* imidase was obtained. Then homology modeling and molecular docking were used to understand this question. The *Tetraodon nigroviridis* imidase structure exhibit three major differences with *Agrobacterium tumefaciens* hydantoinase: (1) they have zinc only in α - site coordinated by H62 N ϵ 2, H64 N ϵ 2, D321 O δ 1 and HOH1. (2) they have open β - site and free H187 and H243. (3) side chain of K154 without post modification was shorter than Kcx148 in hydantoinase. Molecular docking of 5-hydantoinacetic acid and parabanic acid into *Tetraodon nigroviridis* imidase showed that both of them can enter the active site, but had different orientations than in *Agrobacterium tumefaciens* hydantoinase. Enzymatic assays showed that *Agrobacterium tumefaciens* hydantoinase did hydrolyze the 5-hydantoinacetic acid and parabanic acid. For *Tetraodon nigroviridis* imidase, 5-hydantoinacetic acid and parabanic acid are not the substrates, but competitive inhibitors. A reasonable explanation is that compounds tended to the open β - site and formed weak hydrogen bonds with free residues, K154, H187 and H243.

Reference

Abendroth, J., Niegind, K., and Schomburg, D. X-ray structure of a dihydropyrimidinase from *Thermus* sp. at 1.3 Å resolution. *J. Mol. Biol.* 2002, 320, 143-156.

Abendroth, J., Niefind, K., May, O., Siemann, M., Syldatk, C., and Schomburg, D. The structure of L-hydantoinase from *Arthobacter aurescens* leads to an understanding of dihydropyrimidinase substrate and enantio specificity. *Biochemistry* 2002, 41, 8589-8597.

Benini, S., Ciurli, S., Nolting, H.F., and Mangani, S. X-ray absorption spectroscopy study of native and phenylphosphorodiamidate-inhibited *Bacillus pasteurii* urease.

Eur. J. Biochem. 1996, 239, 61-66.

Benini, S., Rypniewski, W.R., Wilson, K.S., Ciurli, S., and Mangain, S. Structure-based rationalization of urease inhibition by phosphate: novel insights into the enzyme mechanism.

J. Biol. Inorg. Chem. 2001, 6, 778-790.

Benini, S., Rypniewski, W.R., Wilson, K.S., Miletto, S., Ciurli, S., and Mangani, S. A new proposal for urease mechanism based on the crystal structures of native and inhibited enzyme from *Bacillus pasteurii*: why urea hydrolysis costs two nickels. *Structure* 1999, 7, 205-216.

Bernheim, F., and Bernheim, M.L.C. The hydrolysis of hydantoin by various tissue. *J. Bio. Chem.* 1946, 163, 683-685.

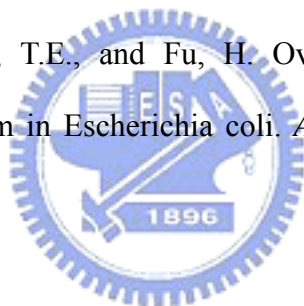
Brooks, K.P., Kim, B.D., and Sander, E.G. Dihydropyrimidine amidohydrolase is a zinc metalloenzyme. *Biochim Biophys Acta.* 1979, 570, 213-214.

Brooks, K.P., Jones, E.A., Kim, B.D., and Sander, E.G. Bovine liver dihydropyrimidine amidohydrolase: purification, properties and characterization as a zinc metalloenzyme. *Arch. Biochem. Biophys.* 1983, 226, 469-483.

Buchanan, K., Burton, S.G., Dorrington, R.A., Matcher, G.F., Skepu, Z. A novel *Pseudomonas putida* strain with high levels of hydantoin-converting activity, producing L-amino acids. *J. Mol. Catal. B* 2001, 11, 397-406.

Campbell, Jr. L.L. Reductive degradation of pyrimidines. IV. Purification and properties of dihydrouracil hydase. *J. Biol. Chem.* 1958, 233, 1236-1240.

Chao, Y.P., Chiang, C.J., Lo, T.E., and Fu, H. Overproduction of D-hydantoinase and carbamoylase in a soluble form in *Escherichia coli*. *Appl. Microbiol. Biotechnol.* 2000, 54, 348-353.



Cheon, Y.H., Kim, H.S., Han, K.H. Abendroth, J., Niefind, K., Schomburg, D., Wang, J., and Kim, Y. Crystal structure of D-hydantoinase from *Bacillus stearothermophilus*: insight into the stereochemistry of enantioselectivity. *Biochemistry* 2002, 41, 9410-9417.

Drauz, K. Chiral amino acids: a versatile tool in the synthesis of pharmaceuticals and fine chemicals. *Chimia* 1997, 51, 310-314.

Eadie, G.S., Bernheim, F., and Bernheim, M.L.C. The partial purification and properties of animal and plant hydantoinases. *J. Bio. Chem.* 1949, 181, 449-458.

Fink, R.M., Cline, R.E., and Koch, H.M.G. Chromatographic detection of pyrimidine reduction products: microbiological application. *Fed. Proc.* 1954, 13, 207-208.

Gasteiger, J., Sadowski, J., Schuur, J., Selzer, P., Steinhauer, L., and Steinhauer, V. Chemical information in 3D-space. *J. Chem. Inf. Comput. Sci.* 31, 1030-1037.

van Gennip, A.H., Abeling, N.G.G.M., Vreken, P., and Kuilenburg, A.B.P. van. Inborn errors of pyrimidine degradation: clinical, biochemical and molecular aspects. *J. Inherited. Metab. Dis.* 1997, 20, 203-213.

Gerlt, J.A., and Raushel, F.M. Evolution of function in $(\beta/\alpha)_8$ -barrel enzymes. *Curr. Opin. Chem. Biol.* 2003, 7, 252-264.

Guex, N., and Peitsch, M.C. Swiss-Model and the Swiss-PdbViewer: an environment for comparative protein modeling. *Electrophoresis* 1997, 18, 2714-2723.

Hasinoff, B.B. The hydrolysis-activation of the doxorubicin cardioprotective agent ICRF-187 ((+)-1,2-bis(3,5-dioxopiperazin-1-yl)propane). *Drug Metab. Dispos.* 1990, 18, 344-349.

Hasinoff, B.B., Venkataram, S., Singh, M., and Kuschak, T.I. Metabolism of the cardioprotective agents dexrazoxane (ICRF-187) and levrazoxane (ICRF-186) by the isolated hepatocyte. *Xenobiotica* 1994, 24, 977-987.

Hayashi, K., Kidouchi, K., Sumi, S., Mizokami, M., Orito, E., Kumada, K., Ueda, R., and Wada, Y. Possible prediction of adverse reactions to pyrimidine chemotherapy from urinary pyrimidine levels and a case of asymptomatic adult dihydropyrimidinuria. *Clin. Cancer Res.*

1996, 2, 1937-1941.

Huang, C.Y., Chao, Y.P., and Yang, Y.S. Purification of industrial hydantoinase in one step chromatographic step without affinity tag. *Protein Expr. Purif.* 2003, 30, 134-139.

Huang, C.Y., and Yang, Y.S. The role of metal on imide hydrolysis: metal content and pH profiles of metal ion-replaced mammalian imidase. *Biochem. Biophys. Res. Commun.* 2002, 297, 1027-1032.

Huang, C.Y., and Yang, Y.S. A novel cold-adapted imidase from fish *Oreochromis niloticus* that catalyzes hydrolysis of maleimide. *Biochem. Biophys. Res. Commun.* 2003, 312, 467-472.

Hull, W.E., Port, R.E., Herrmann, R., Britsch, B., and Kunz, W. Metabolites of 5-fluorouracil in plasma and urine, as monitored by ^{19}F nuclear magnetic resonance spectroscopy, for patients receiving chemotherapy with or without methotrexate pretreatment. *Cancer Res.* 1988, 48, 1680-1688.

Ishikawa, T., Mukohara, Y., Watabe, K., Kobayashi, S., and Nakamura, H. Microbial conversion of DL-5-substituted hydantoins to the corresponding L-amino acids by *Bacillus stearothermophilus* NS1122A. *Biosci. i Biotechnol. Biochem.* 1994, 58, 265-270.

Jabri, E., Carr, M.B., Hausinger, R.P., and Karplus, P.A. The crystal structure of urease from *Klebsiella aerogenes*. *Science* 1995, 268, 998-1004.

Jones, G., Willett, P., Glen R. C., Leach, A. R., and Taylor, R. Development and validation of genetic algorithm for flexible docking. *J. Mol. Biol.* 1997, 267, 727-748

Clemente-Jimenez, J.M., Martinez-Rogriguez, S., Mingorance-Cazorla, L., De La Escalera-Hueso, S., Las Heras-Vazquez, F.J., Rodriguez-Vico, F. Catalytic analysis of a recombinant D-hydantoinase from *Agrobacterium Tumefaciens*. *Biotechnol. Lett.* 2003, 25, 1067–1073.

Kagabu, S., Moriya, K., Shibuya, K., Hattori, Y., Tsuboi, S., and Shiokawa, K. 1-(6-Halonicotinyl)-2-nitromethylene-imidaxolidines as potential new insecticides. *Biosci. Biotechnol. Biochem.* 1992, 56, 362-363.

Kikugawa, M., Kaneko, M., Fujimoto-Sakata, S, Maeda, M., Kawasaki, K., Takagi, T., and Tamaki, N. Purification, characterization and inhibition of dihydropyrimidinase from rat liver. *Eur. J. Biochem.* 1994, 219, 393-399.

Kim, G.J., and Kim, H.S. C-terminal regions of D-hydantoinases are nonessential for catalysis, but affect the oligomeric structure. *Biochem. Biophys. Res. Commun.* 1998, 243, 96–100.

Kim, G.J., Lee, D.E., and Kim, H.S. Functional expression and characterization of the two cyclic amidohydrolase enzymes, allantoinase and a novel phenylhydantoinase, from *Escherichia coli*. *J. Bacteriol.* 2000, 182, 7021-8.

Krakewska, B., and Zaborska, W. The effect of phosphate buffer in the range of pH 5.80–8.07 on jack bean urease activity. *J. Mol. Catal. B* 1999, 6, 75-81.

LaRue, T.A., and Spencer, J.T.F. The utilization of purines and pyrimidines by yeasts. *Can. J. Microbiol.* 1968, 14, 79-86.

Lee, S.G., Lee, D.C., and Kim, H.S. Purification and characterization of thermostable D-hydantoinase from thermophilic *Bacillus stearothermophilus* SD1. *Appl. Biochem. Biotechnol.* 1997, 62, 251-266.

Lee, S.G., Lee, D.C., Hong, S.P., Sung, M.H., and Kim, H.S. Thermostable D-hydantoinase from thermophilic *Bacillus stearothermophilus* SD-1: characteristics of purified enzyme. *Appl. Microbiol. Biotechnol.* 1995, 43, 270-276.

May, O., Siemann, M., Siemann, G., and Syldatk, C. The hydantoin amidohydrolase from *Arthrobacter aurescens* DSM 3745 is a zinc metalloenzyme. *J. Mol. Catal. B* 1998, 5, 367-370.

Morin, A., Hummel, W., SchuÈtte, H., and Kula, M.R. Characterization of hydantoinase from *Pseudomonas fluorescens* strain DSM 84. *Biotechnol. Appl. Biochem.* 1986, 8, 564-574.



Moriya, K., Shibuya, K., Hattori, Y., Tsuboi, S., Shiokawa, K., and Kagabu, S. Structural modification of the 6-chloropyridyl moiety in the imidacloprid skeleton: introduction of a five-membered heteroaromatic ring and the resulting insecticidal activity. *Biosci. Biotechnol. Biochem.* 1993, 57, 127-128.

Musiani, F., Arnosi, E., Casadio, R., and Ciurli, S. Structure-based computational study of the catalytic and inhibition mechanisms of urease. *J. Biol. Inorg. Chem.*, 2001, 6, 300-314.

Naguib, F.N.M., Kouni, M.H. el, and Cha, S. Enzymes of uracil catabolism in normal and neoplastic human tissues. *Cancer Res.* 1985, 45, 5405-5412.

Ogawa, J., Honda, M., Soong, C.L., and Shimizu, S. Diversity of cyclic ureide compound-, dihydropyrimidine-, and hydantoin-hydrolyzing enzymes in *Blastobacter sp.* A17p-4. *Biosci. Biotechnol. Biochem.* 1995, 59, 1960-1962.

Ogawa, J., and Shimizu, S. Microbial enzymes: new industrial applications from traditional screening methods. *Trends Biotechnol.* 1999, 17, 13-20.

Ogawa, J., and Shimizu, S. Diversity and versatility of microbial hydantoin transforming enzymes. *J. Mol. Catal. B* 1997, 2, 163-176.

Olivier, R., Fascetti, E., Angelini, L., and Degen, L. Microbial transformation of racemic hydantoins to D-amino acids. *Biotechnol. Bioeng.* 1981, 23, 2173-2183.

Park, J.H., Kim, G.J., Lee, D.C., and Kim, H.S. Purification and characterization of thermostable D-hydantoinase from *Bacillus thermocatenuatus* GH2. *Appl. Biochem. Biotechnol.* 1999, 81, 53-65.

Radha Kishan, K.V., Vohra R.M., Ganesan, K., Agrawa, V., Sharma, V. M., and Sharma, R. Molecular structure of D-hydantoinase from *Bacillus sp.* AR9: Evidence for mercury inhibition. *J. Mol. Biol.* 2005, 347, 95-105.

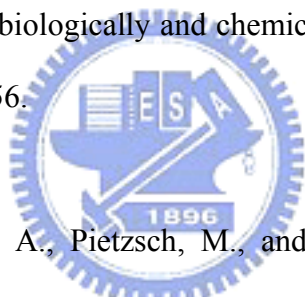
Runser, S., and Meyer, P.C. Purification and biochemical characterization of the hydantoin hydrolyzing enzyme from *Agrobacterium species*. A hydantoinase with no 5,6-dihydropyrimidine amidohydrolase activity. *Eur. J. Biochem.* 1993, 213, 1315-1324.

Sanno, Y., Holzer, M., and Schimpl, R.T. Studies of a mutation affecting pyrimidine degradation in inbred mice. *J. Bio. Chem.* 1970, 245, 5668-5676.

Schwede, T., Kopp, J., Guex, N., and Peitsch, M.C. Swiss-Model: an automated protein homology-modeling server. *Nucleic Acids Res.* 2003, 31, 3381–3385.

Shevchenko, A., Jensen, O.N., Podtelejnikov, A.V., Sagliocco, F., Wilm, M., Vorm, O., Mortensen, P., Shevchenko, A., Boucherie, H., Mann, M. Linking genome and proteome by mass spectrometry: large-scale identification of yeast proteins from two-dimensional gels. *Proc. Natl. Acad. Sci. USA* 93 (25), 14440–14445.

Shimizu, S., Ogawa, J., Kataoka, M., and Kobayashi, M. Screening of novel microbial enzymes for the production of biologically and chemically useful compounds. *Adv. Biochem. Eng. Biotechnol.* 1997. 58, 45-56.



Siemann, M., Alvarado-Marin A., Pietzsch, M., and Syldatk, C. A D-specific hydantoin amidohydrolase: properties of the metalloenzyme purified from *Arthrobacter crystallopoietes*. *J. Mol. Catal. B* 1999, 6, 387-397.

Smith, A.E. and Yamada, E.W., Dihydrouracil dehydrogenase of rat liver, separation of hydrogenase and dehydrogenase activity. *J. Bio. Chem.* 1971, 246, 3610-3617

.

Soong, C.L., Ogawa, J., Honda, M., and Shimizu, S. Cyclic-imide-hydrolyzing activity of D-hydantoinase from *Blastobacter sp.* strain A17p-4. *Appl. Environ. Microbiol.* 1999, 65, 1459-62.

Sumi S., Imaeda, M., Kidouch,i K., Ohba, S., Hamajima, N., Kodama, K., Togari, H., and Wada ,Y. Population and family studies of dihydropyrimidinuria: prevalence, inheritance moe and risk of fluorouracil toxicity. *Am. J. Med. Genet.* 1998, 78, 336-340.

Su, T.M., and Yang, Y.S. Identification, purificaiton, and characterization of a thermophilic imidase from pig liver. *Protein Expr. Purif.* 2000, 19, 289-297.

Syldatk, C., May, O., Altenbuchner, J., Mattes, R., and Siemann, M. Microbial hydantoinases ± industrial enzymes from the origin of life? *Appl. Microbiol. Biotechnol.* 1999, 51, 293-309.

Syldatk, C., MuÈller, R., Siemann, M., and Wagner, F. Microbial and enzymatic production of D-amino acids from DL-5-monosubstituted hydantoins. In: Rozzell, JD, Wagner F (eds) *Biocatalytic production of amino acids and derivatives*. Hanser, NewYork, 1992, pp 75-127.

Syldatk, C., and Pietzsch, M. Hydrolysis and formation of hydantoins. In: Drauz K, Waldmann H (eds) *Enzyme caalysis in organic synthesis*. Verlag Chemie, Weinheim, 1995, pp 409-431.

Takahashi, S., Kii, Y., Kumagai, H., and Yamada, H. Purification, crystallization and properties of hydantoinase from *Pseudomonas striata*. *J. Ferment. Technol.* 1978, 56, 492-498.

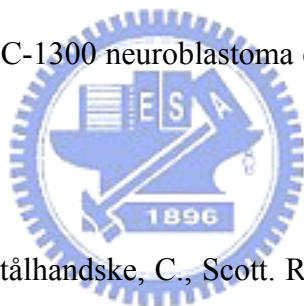
Takahashi, S., Ohashi, T., Kii, Y., and Yamada, H. Microbial transformation of hydantoins to N-carbamoyl-D-amino acids. *J. Ferment. Technol.* 1979, 57, 328-332.

Thoden, J.B., Neal, T.M., Raushel, F.M., and Holden, H.M. Molecular structure of dihydroorotase: a paradigm for catalysis through the use of a binuclear metal center. *Biochemistry* 2001, 40, 6989-6997.

Tramper, J., and Luyben, K.C.A.M. Biotechnologische produktie van D-(-)-4-hydroxyfenylfycine. *PT/Procestechiek* 1984, 39, 61-67.

Tsai, C.S., and Axelrod, B. Catabolism of pyrimidines in rape seedlings. *Plant. Physiol.* 1965, 40, 39-44.

Tuchman, M., O'Dea, R.F., Ramnaraine, M.L.R., and Mirkain, B.L. Pyrimidine base degradation in cultured murine C-1300 neuroblastoma cells and in situ tumors. *J. Clin. Invest.* 1988, 81, 425-430.



Yamaguchi, K., Cospers, N.J., Stålhandske, C., Scott, R.A., Pearson, M.A., Karplus, P.A., and Hausinger, R.P. Characterization of metal-substituted *Klebsiella aerogenes* urease. *J. Biol. Inorg. Chem.* 1999, 4, 468-477.

Yang, J.M., and Chen, C.C. GEMDOCK: A generic evolutionary method for molecular docking. *Proteins* 2004, 55, 288-304.

Yang, J.M. Development and evaluation of a generic evolutionary method for protein-ligand docking. *J. Comput. Chem.* 2004, 25, 843-857.

Yang, Y.S., Ramaswamy, S., and Jakoby, W.B. Rat liver imidase. *J. Bio. Chem.* 1993, 268, 10870-10875.

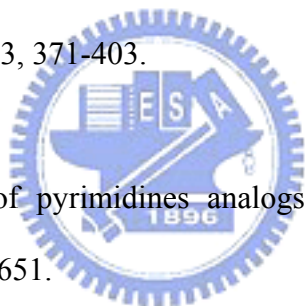
Vanhooke, J.L., Benning, M.M., Raushel, F.M., and Holden, H.M. Three-dimensional structure of the zinc containing phosphotriesterase with the bound substrate analogue diethyl 4-methylbenzylphosphonate. *Biochemistry* 1996, 35, 6020-6025.

Vogels, G.D., and van der Drift, C. Degradation of purines and pyrimidines in microorganism. *Bacteriol. Rev.* 1976, 40, 403-468.

Wallach, D.P., and Grisolia, S. The purification and properties of hydroxypyrimidine hydrolase. *J. Biol. Chem.* 1957, 226, 277-288.

Wasternack, C. Degradation of pyrimidines - enzymes, localization and role in metabolism. *Biochem. Physiol. Pfl.* 1978, 173, 371-403.

Wasternack, C. Degradation of pyrimidines analogs – pathways and mutual influences. *Pharmacol. Ther.* 1980, 8, 629-651.



Watabe, K., Ishikawa, T., Mukohara, Y., and Nakamura, H. Purification and characterization of the hydantoin racemase of *Pseudomonas* sp. strain NS671 expressed in *Escherichia coli*. *J. Bacteriol.* 1992, 174, 3461-3466.

Xu, Z., Liu, Y., Yang, Y., Jiang, W., Arnold, E., and Ding, J. Crystal structure of D-Hydantoinase from *Burkholderia pickettii* at a resolution of 2.7 Angstroms: insights into the molecular basis of enzyme thermostability. *J. Bacteriol.* 2003, 185, 4038-4049.

Xu, G., and West, T.P. Characterization of dihydroxypyrimidinase from *Pseudomonas stutzeri*. *Arch. Microbiol.* 1994, 161, 70-74.

Table 1. Summary of purification of imidase from fish liver (*Oreochromis niloticus*)^a

Step	Volume (ml)	Total Activity (μ mol/min)	Total Protein (mg)	Specific Activity (μ mol/min/mg)	Yield (%)	Fold of purification
Extract	370	1180.4	35768	0.03	100	1
35% Salt out	360	1006.2	17054	0.06	85	1.8
60% Salt out	50	873.5	6065	0.14	74	4.4
Octyl Sepharose	15	501.9	529.5	0.95	43	28.7
Chelating Sephacel	10	297.4	15.4	19.3	25	586
Hydroxyapatite	2	153.1	2.82	54	13	1642
HiTrap Q Sepharose	0.5	106.1	1.22	87	9	2630

^a All procedures for purification of fish liver imidase were described in “2.4 protein purification” and the assay was made according to “2.2 enzyme standard assay”.

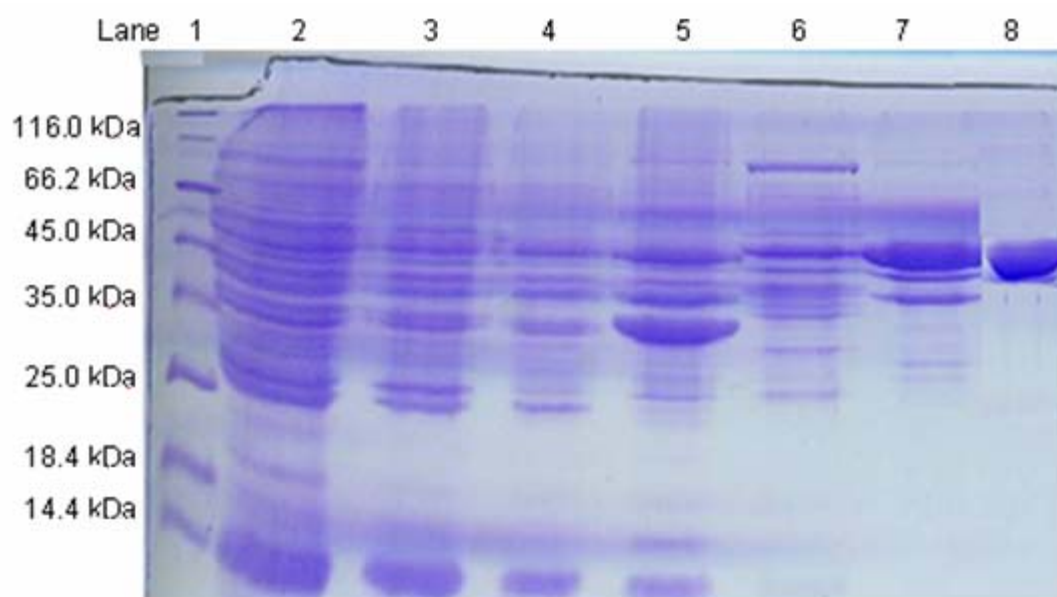


Figure 1. The purity of fish liver (*Oreochromis niloticus*) imidase.

SDS-PAGE (12%) of purified fish liver imidase (56K). Lane 1, protein standard (from Pharmacia) with size noted in; lane 2, extract; lane 3, 35% salt out; lane 4, 60% salt out; lane 5, Octyl Sepharose; lane 6, Chelating Sephacel; lane 7, Hydroxyapatite; lane 8, HiTrap Q Sepharose.

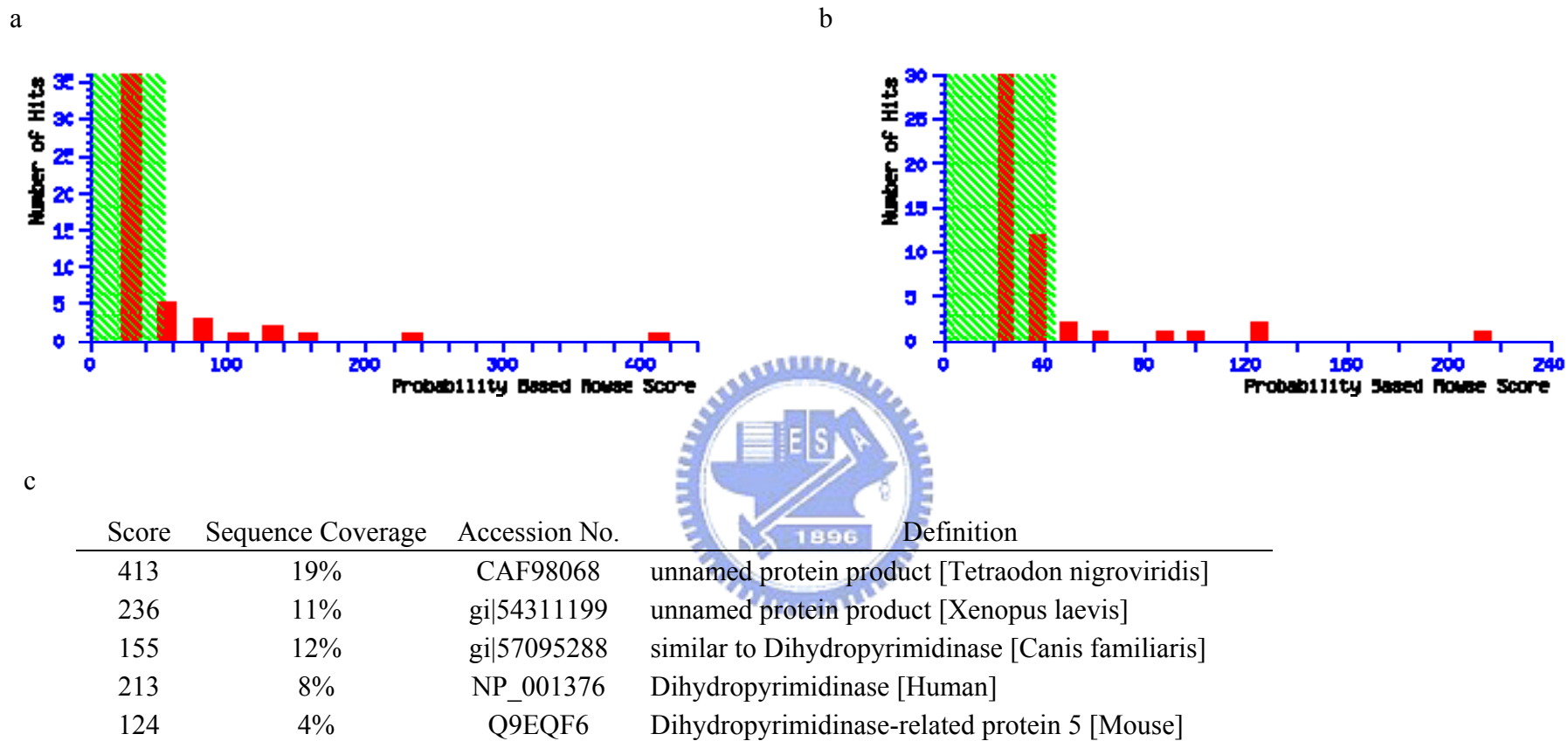
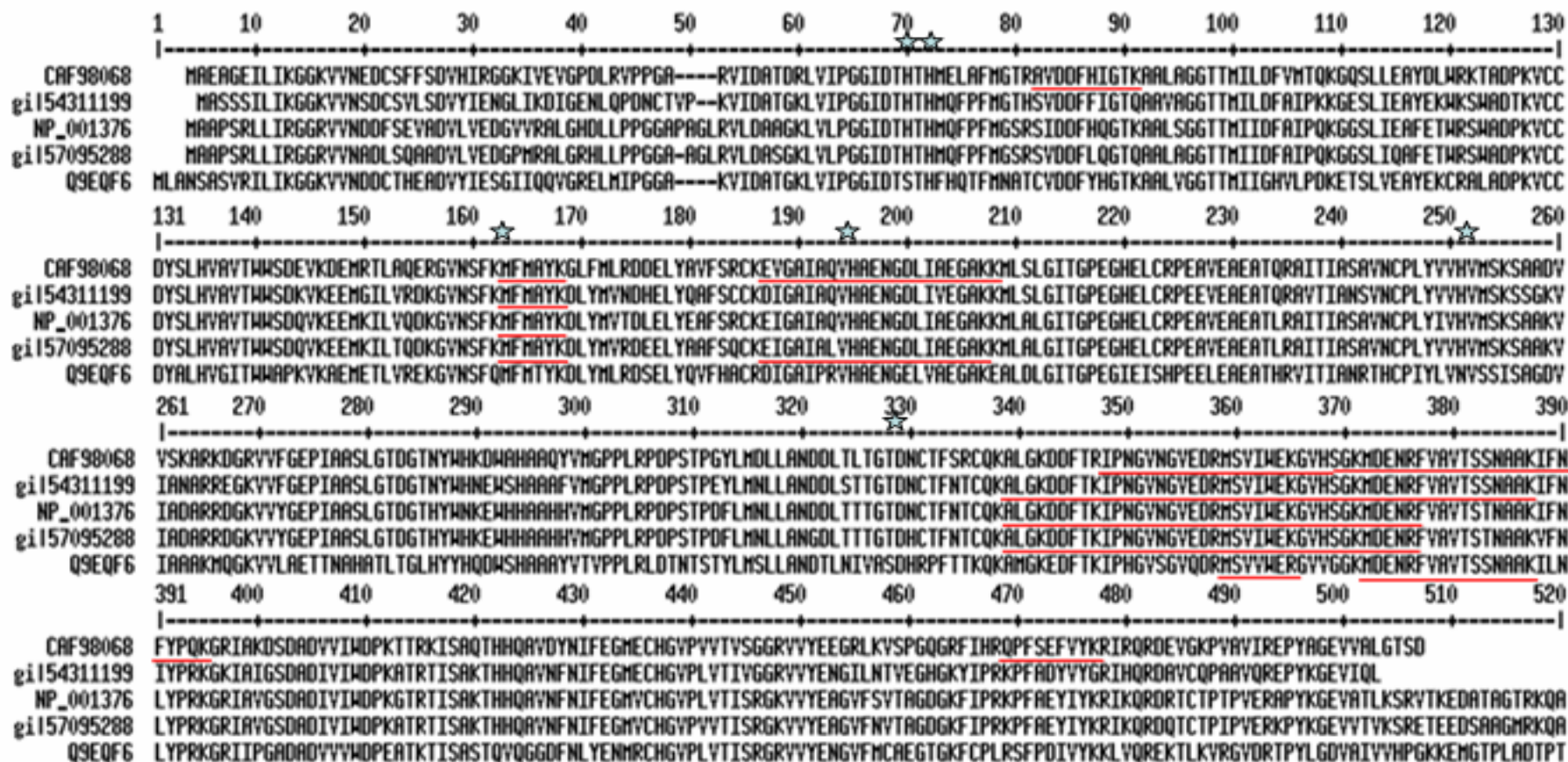


Figure 2. fish liver (*Oreochromis niloticus*) imidase was analyzed using LC-ESI-MS.

The results were correlated with the sequence database using the NCBI (a) and SwissProt (b) database and analyzed by Mascot software.

(c) protein summary report.



SeqA Name	Len(aa)	SeqB Name	Len(aa)	Score
1 NP_001376	519	2 CAF98068	500	73
1 NP_001376	519	3 gi 54311199	497	78
1 NP_001376	519	4 gi 57095288	518	92
1 NP_001376	519	5 Q9EQF6	564	57

Figure 3. Sequence alignment of various imidase correlated with the sequence database by Mascot software.

The sequences of *Tetraodon nigroviridis* unnamed protein (CAF98068), *Xenopus laevis* unnamed protein (gi|54311199), human dihydropyrimidinase (NP_001376), putative *Canis familiaris* dihydropyrimidinase (gi|57095288) and mouse dihydropyrimidinase related protein-5 (Q9EQF6) are shown aligned by ClustalW. The letters in underline represent the matched peptide fragments. The stars represent the six conserved metal binding residues (four histidines, one carboxylated lysine, and one aspartic acid).




```

1  atg gcagaagccggcgagatcctgattaaaggaggcaagggtggaacgaggactgctcctcttcagcgacgttcacatcagaggagggt
   H A E A G E I L I K G G K V U N E D C S F F S D V H I R G G
91  aaaatagtggaagtcggcctgatcttcgggtcccgcggggcccgagtgatcgatcgaccgacagactggtgatcccgaggaggatc
   K I U E U G P D L R U P P G A R U I D A T D R L V I P G G I
181 gacacgcacacgcacatggagctggcggtcatgggcaccagagctgtggacgacttcacatcgggaccaaggccctctggcaggagga
   D T H T H H E L A F M G T R A U D D F H I G T K A A L A G G
271 accacaatgatcctggactttgtcatgaccagaagggtcagtcctcctggaggcctacgacctctggcgtaaagcggctgaccccaag
   T T M I L D F V M T Q K G Q S L L E A Y D L W R K T A D P K
361 gtttctgcgactactctctgcacgtcgcgctcacatgggtggagcaccagggtcaaggacgaaatgcggaccctggcccaggagaggggg
   U C C D Y S L H U A U T W W S D Q U K D E M R T L A Q E R G
451 gteaactcttcaagatggttcagcctacaaaggcctggtcatgtcggggacgatgagctgtacgccctctctcccactgcaaggag
   U N S F K M F H A Y K G L F H L R D D E L Y A U F S H C K E
541 gttggagccatcgtcagggtcacgctgagaacgggtgatctgatcgcagagggggccaagaagatgtcgtcgttggcattcacggggcct
   V G A I A Q V H A E N G D L I A E G A K K M L S L G I T G P
631 gagggtcatgagctgtgtcgcaccagaggcgggtggaggccgagccaccagcgcgccatcaccatcgccagcggcgtcaactgtccctc
   E G H E L C R P E A V E A E A T Q R A I T I A S A V N C P L
721 tacgtggtccacgtcatgagcaaatctgcagccgacgtggtgtccaaggcccgaagatggcctgtggtgttggagagcccatcgca
   Y U U H U M S K S A A D U V S K A R K D G R U V F G E P I A
811 gcctcactgggcacagatgggaccaactactggcacaaggactgggccatgcagctcagatgtcatggggccccctccgccctgac
   A S L G T D G T N Y W H K D W A H A A Q Y U M G P P L R P D
901 cccagcactcccggatctcatggacctcctggccaacgatgatctcacgttgacggggaccgacaactgcacctttcttaggtgccag
   P S T P G Y L H D L L A N D D L T L T G T D N C T F S R C Q
991 aaagctctgggcaaggacgacttcaccaggattcccaacggagtcacagagtgaggagcaggatgtccgtcatctgggagaaaggagtg
   K A L G K D D F T R I P N G U N G V E D R M S U I V E K G U
1081 cacagcggcaaaatggacgagaacagatttggtggcgttacagagcagcaacgcagcaaaaaatcttcaactctaccgcagaaggccga
   H S G K M D E N R F V A U T S S N A A K I F N F Y P Q K G R
1171 atagccaaagactcggacgtgacgtggttatatgggacccccaaaacaagaagaaaatctcagcgcagacgcaccaccaggctgtggac
   I A K D S D A D U U I W D P K T T R K I S A Q T H H Q A U D
1261 tacaacatcttcgagggcattggagtgacggcgttcccggtgacgctcaccagggcagagtggttatgaggaggccggcgtgaa
   Y N I F E G H E C H G U P U U T U S R G R U U Y E E G R L K
1351 gtgtcggccggcaggcaggttcacacagacagcccttctccgaattgtctacaagaggattcccaaggagcaggttaggcaag
   U S P G Q G R F I H R Q P F S E F U Y K R I R Q R D E U G K
1441 cctgccgtgtgatcagagagccctacgcaggcaggtcggttctctgggaacgtctgactga
   P A A V I R E P Y A G E U V A L G T S D -

```

Figure 4. Nucleotide sequence and deduced amino acid sequence.

A pair of primers, fDHP N-ter (5'-atggcagaagccggcgagatc-3') and fDHP C-ter (5'-tcagtcagacgttcccagagcaac-3'), was designed. After PCR, the full-length cDNA of imidase was obtained. The complete nucleotides of fish imidase contained 1503 bp and encoded 500 amino acids. The letters in shadow indicated the start codon (ATG), in “-” indicated the stop codon (TGA) and in red indicated the conserved metal binding residues in the active site.

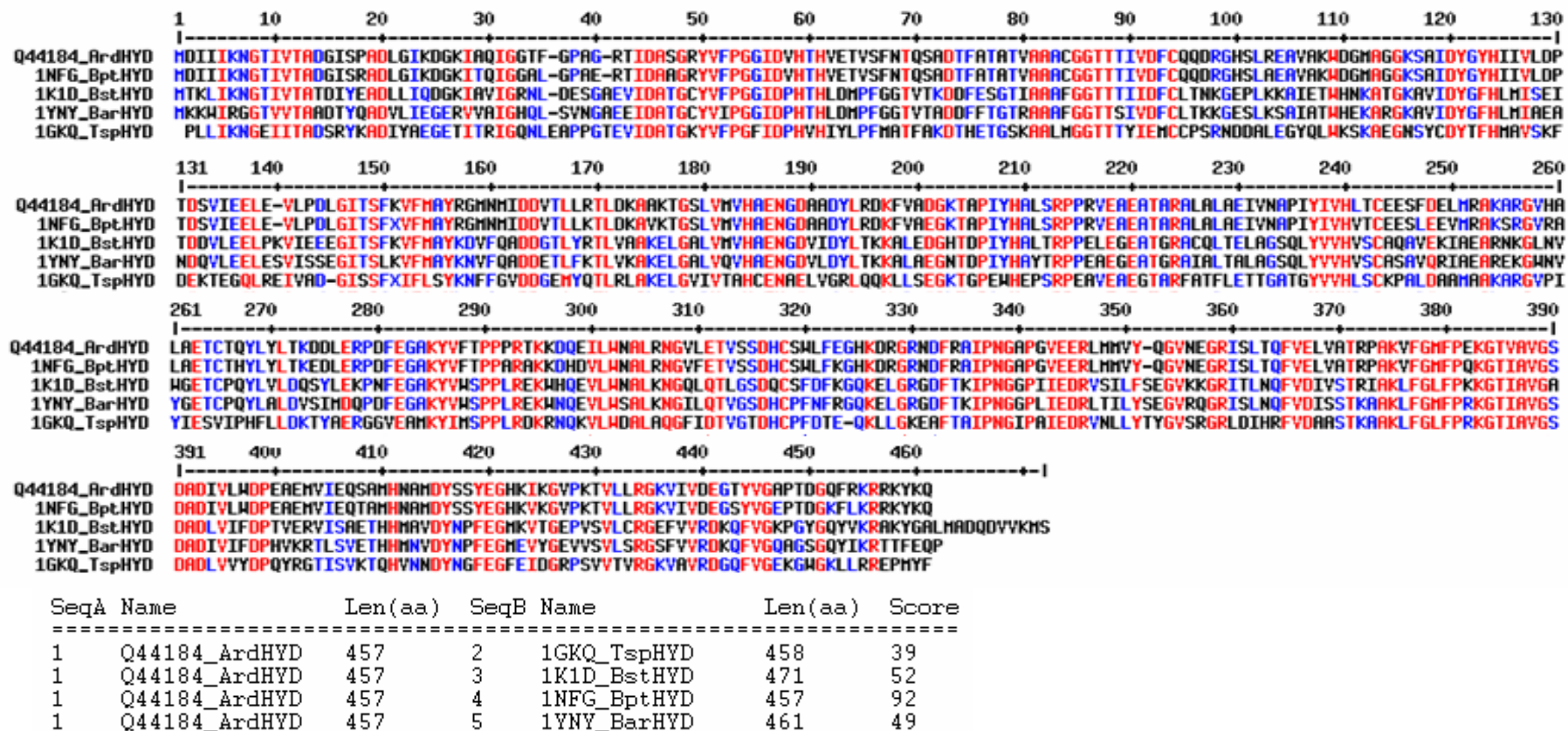
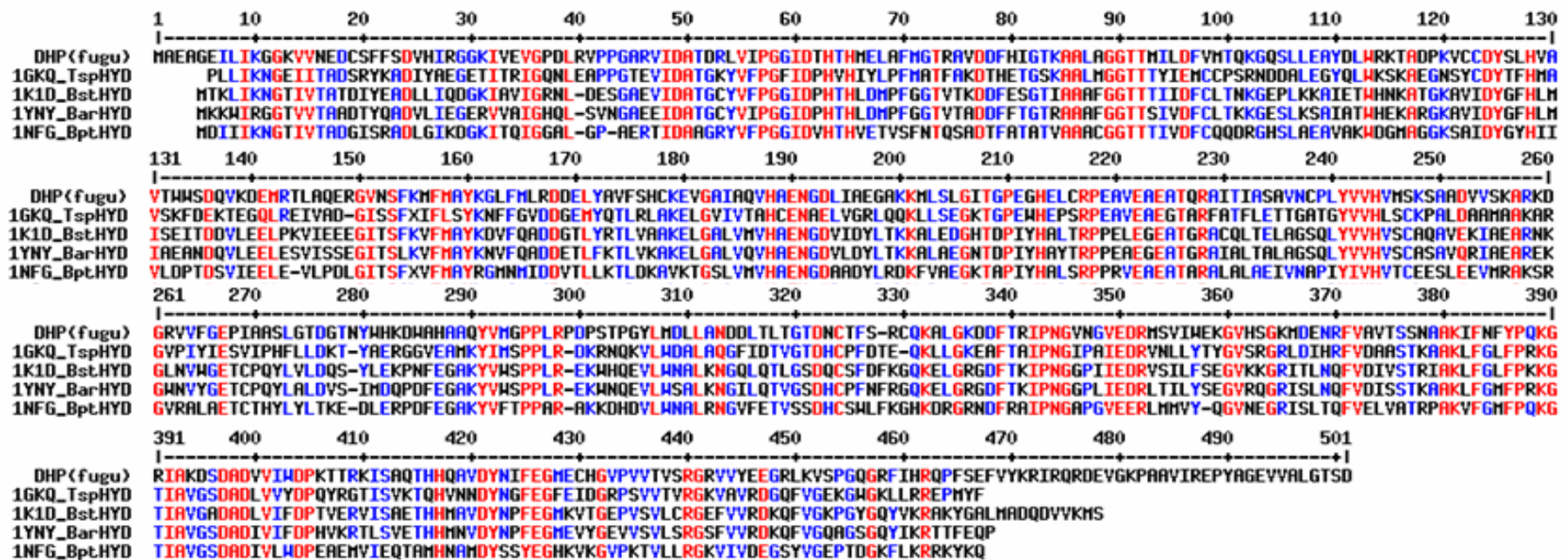


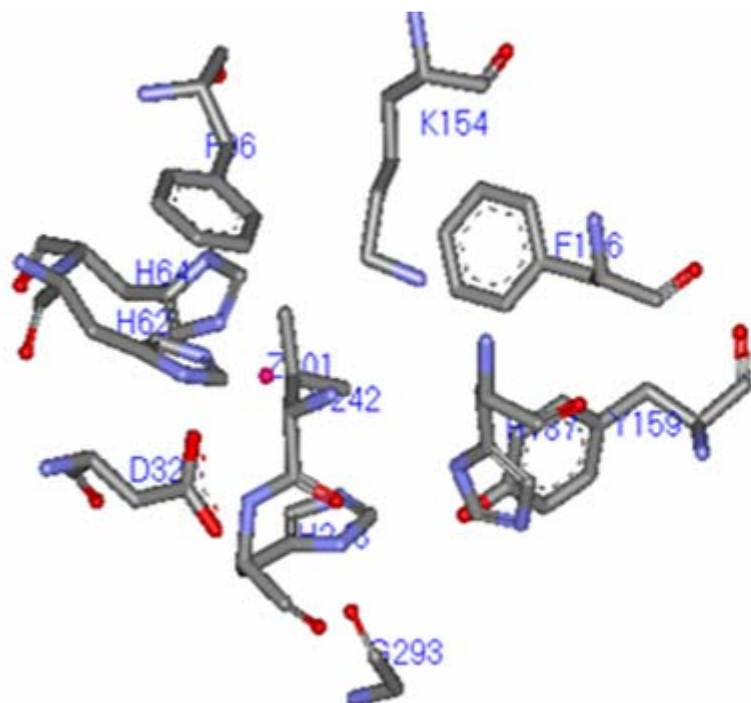
Figure 5. Sequence alignment. The sequences of hydantoinase from *Agrobacterium tumefaciens* (Q44184), *Thermus* sp. (1GKQ), *Bacillus stearothermophilus* (1K1D), *Burkholderia pickettii* (1NFG) and *Bacillus* sp. AR9 (1YNY) are shown aligned by ClustalW.



SeqA Name	Len(aa)	SeqB Name	Len(aa)	Score
1 DHP_fugu	500	2 1GKQ_TspHYD	458	39
1 DHP_fugu	500	3 1K1D_BstHYD	471	41
1 DHP_fugu	500	4 1NFG_BptHYD	457	36
1 DHP_fugu	500	5 1YNY_BarHYD	461	42

Figure 6. Sequence alignment. The sequences of hydantoinase from *Tetraodon nigroviridis* clone, *Thermus* sp. (1GKQ), *Bacillus stearothermophilus* (1K1D), *Burkholderia pickettii* (1NFG) and *Bacillus* sp. AR9 (1YNY) are shown aligned by ClustalW.

a



b

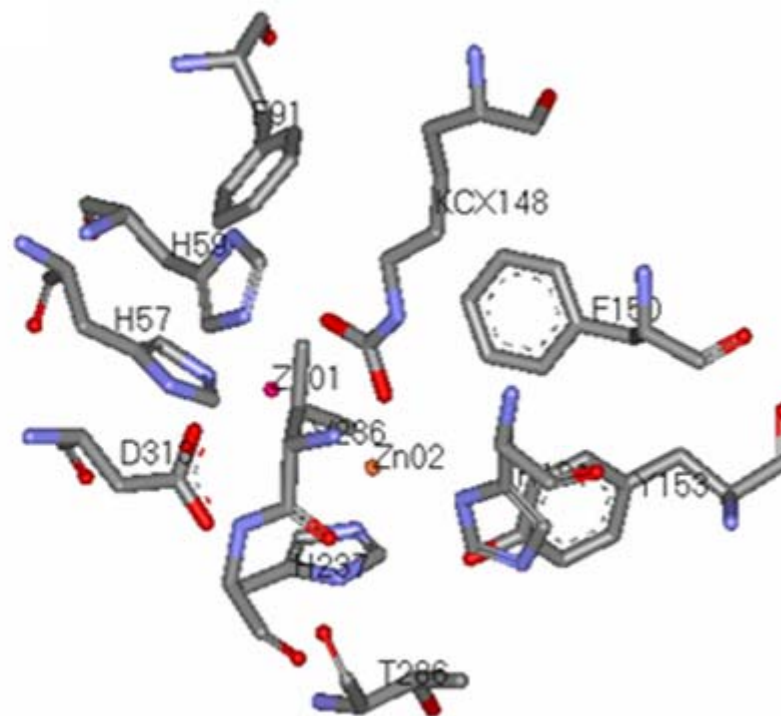
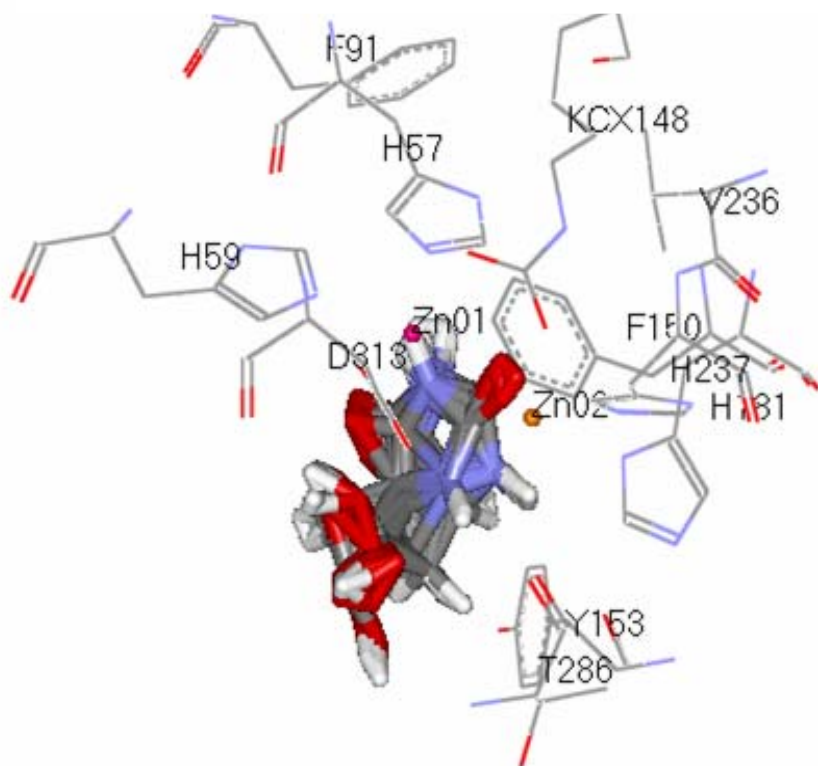


Figure 7. Homology Modeling. a) *Tetraodon nigroviridis* imidase structure was modeled used *Bacillus* sp. AR 9 (PDB code 1YNY) as template. α - zinc is coordinated by H62 N ϵ 2, H64 N ϵ 2, D321 O δ 1 and HOH1. b) *Agrobacterium tumefaciens* hydantoinase structure was modeled used *Burkholderia pickettii* (1NFG) as template. α - zinc is coordinated by H57 N ϵ 2, H59 N ϵ 2, Kcx148 Ox2 and D313 O δ 1. β -zinc is coordinated by Kcx148 Ox1,H181 N δ 1, and H237 N ϵ 2.

a



b

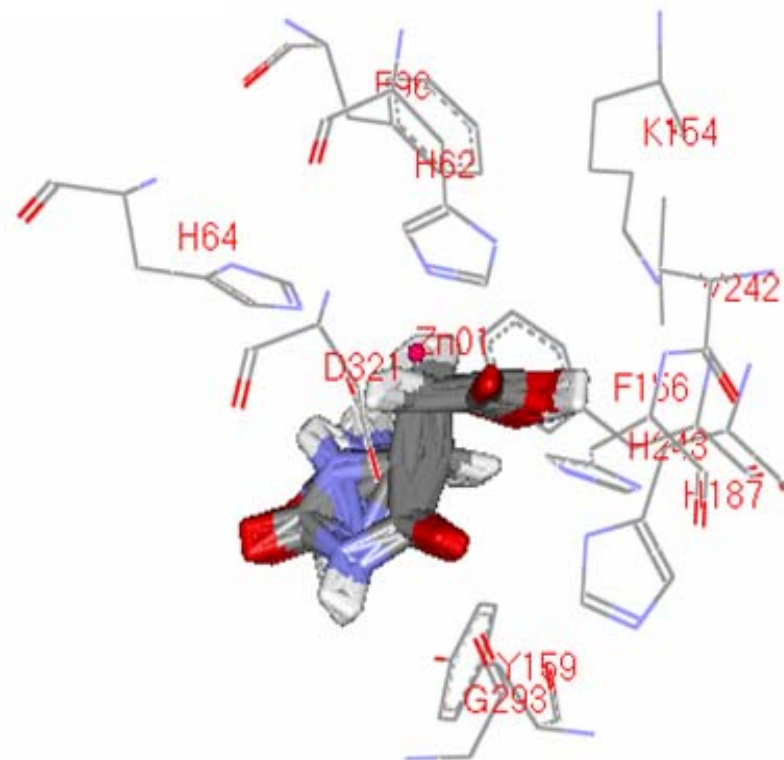


Figure 8. GOLD modeling of 5-hydantoinic acid binding. a) 5-hydantoinic acid can enter the active site of *Agrobacterium tumefaciens* hydantoinase structure and imide ring posited near the bimetal bridged hydroxyl ion. b) 5-hydantoinic acid also can enter the active site of *Tetraodon nigroviridis* imidase structure, but imide ring was swing farther out of the metal ion.

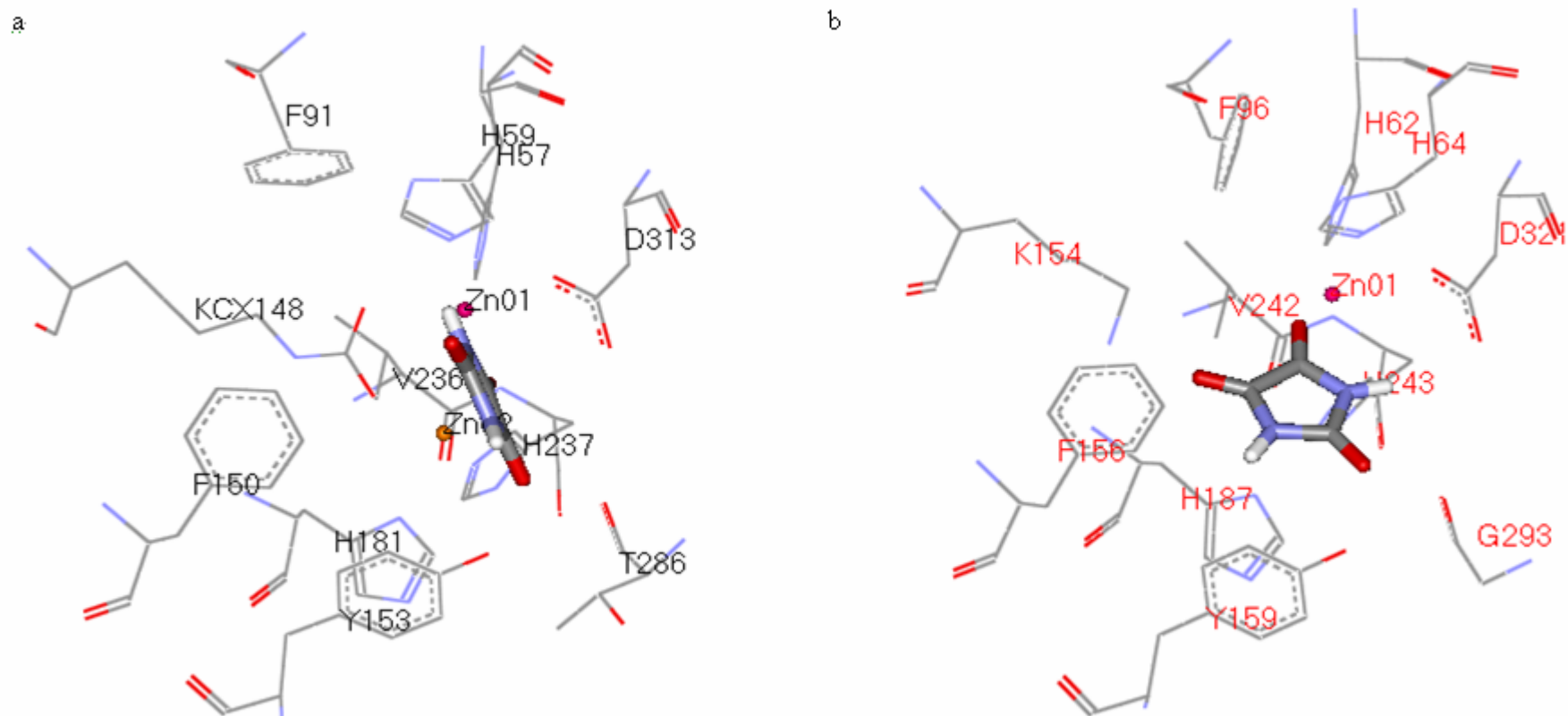


Figure 9. GOLD modeling of parabanic acid binding. a) parabanic acid can enter the active site of *Agrobacterium tumefaciens* hydantoinase structure and imide ring posited near the bimetal bridged hydroxyl ion. b) parabanic acid also can enter the active site of *Tetraodon nigroviridis* imidase structure, but had a different orientation to hydantoinase. This may reflect the recognition of imide hydrolysis.

Table 2. Rate constants of various imidasases using 5-Hydantoinacetic acid and Parabanic acid as substrate^a

	5-hydantoinacetic acid			parabanic acid		
	K_m^b (mM)	V_{max}^b ($\mu\text{mol}/\text{min}/\text{mg}$)	V_{max}/K_m	K_m^c (mM)	V_{max}^c ($\mu\text{mol}/\text{min}/\text{mg}$)	V_{max}/K_m
<i>Agrobacterium tumefaciens</i> hydantoinase	0.6 ± 0.06	15.8 ± 2.51	26	25.33 ± 2.2	65.63 ± 3.64	2.6
<i>Oreochromis niloticus</i> imidase	ND ^d	ND ^d	ND ^d	ND ^d	ND ^d	ND ^b
pig liver imidase	ND ^d	ND ^d	ND ^d	ND ^d	ND ^d	ND ^b

^a The assay were measured at 25°C in 100 mM Bis-Tris propane at pH 7.0 and using 5-Hydantoinacetic acid and Parabanic acid as substrate.

The kinetic constants were obtained from SigmaPlot.

^b A change in A240 of 0.1 represents the hydrolysis of 1 mol of 5-hydantoinacetic acid.

^c A change in A339 of 0.028 represents the hydrolysis of 1 mol of parabanic acid.

^d Not determined due to undetectable or low level of activity.

Table 3. Inhibitory Activities of 5-Hydantoinacetic acid and Parabanic acid^a

	5-hydantoinacetic acid			parabanic acid		
	K_m^b (mM)	V_{max}^b ($\mu\text{mol}/\text{min}/\text{mg}$)	K_i^b (mM)	K_m^c (mM)	V_{max}^c ($\mu\text{mol}/\text{min}/\text{mg}$)	K_i^c (mM)
<i>Oreochromis niloticus</i> imidase	0.48 ± 0.03	58 ± 1.45	44.93 ± 2.1	1.96 ± 0.22	12.1 ± 0.67	35.23 ± 0.5
pig liver imidase	0.44 ± 0.04	25.49 ± 0.83	15.62 ± 0.08	1.11 ± 0.1	15.18 ± 0.51	14.98 ± 0.92

^aThe kinetic constants were obtained from SigmaPlot.

^bInhibitory activity of 5- hydantoinacetic acid was measured at 25°C in 100 mM Bis-Tris propane at pH 7.0 using phthalimide as substrate.

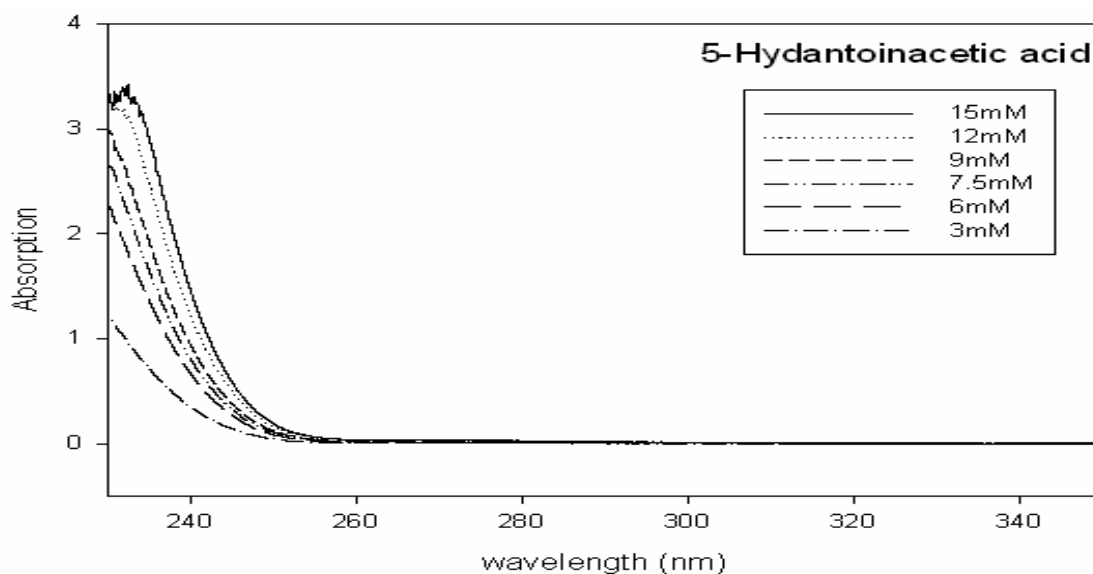
A change in A298 of 2.26 represents the hydrolysis of 1 mol of the substrate.

^cInhibitory activity of parabanic acid was measured at 25°C in 100 mM Bis-Tris propane at pH 7.0 using 3-imoinisoindolinone as substrate.

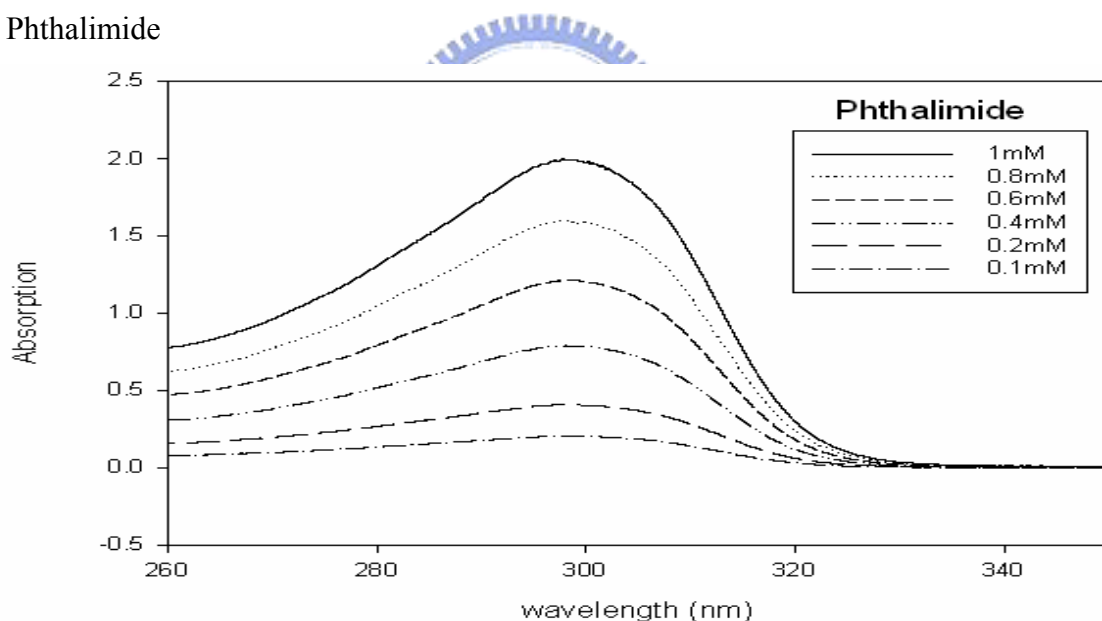
A change in A350 of 0.15 represents the hydrolysis of 1 mol of the substrate.

Appendix

a. 5-Hydantoinacetic acid



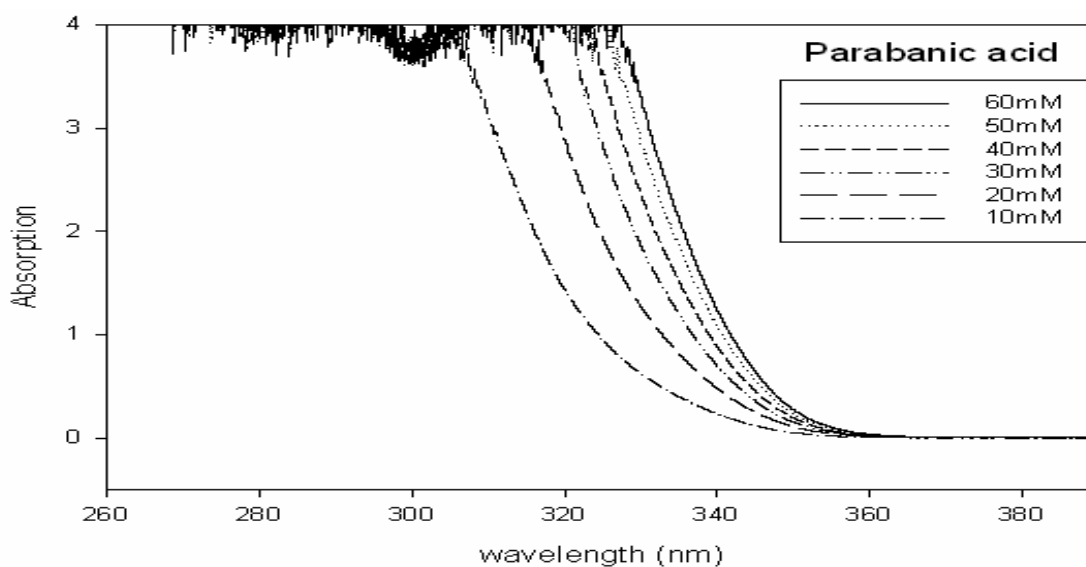
b. Phthalimide



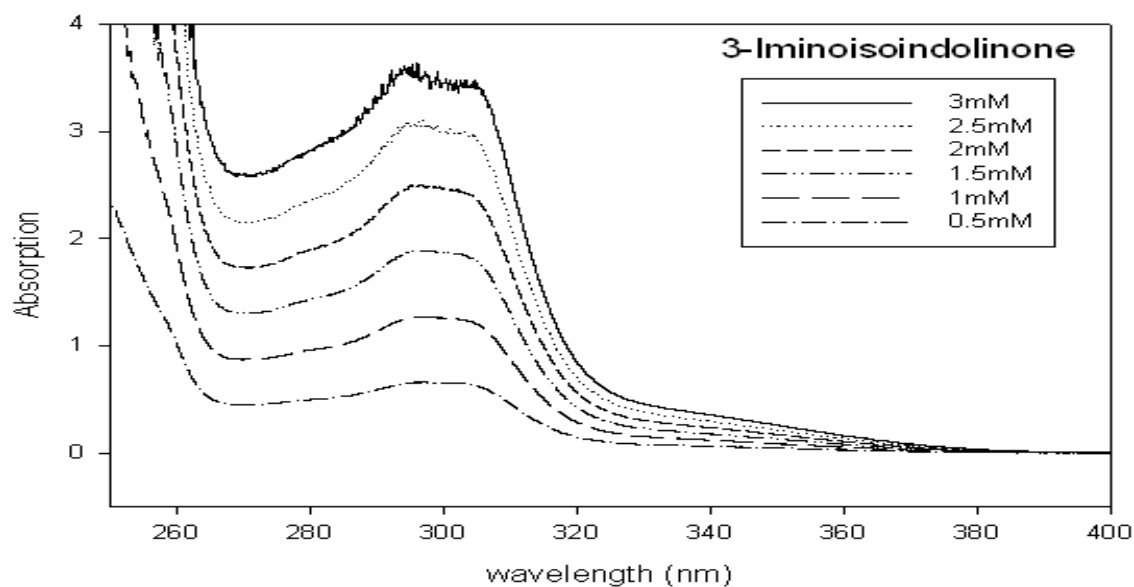
A1. Wavelength scan of a) 5-Hydantoinacetic acid and b) Phthalimide .

1) Substrate activity of 5-hydantoinacetic acid were measured at 25°C in 100 mM Bis-Tris propane(pH 7). A change in A₂₄₀ of 0.1 represents the hydrolysis of 1 mol of 5-hydantoinacetic acid. 2) Inhibitory activity of 5-hydantoinacetic acid was measured at 25°C in 100 mM Bis-Tris propane at pH 7.0 using phthalimide as substrate. A change in A₂₉₈ of 2.26 represents the hydrolysis of 1 mol of the substrate.

a. Parabanic acid



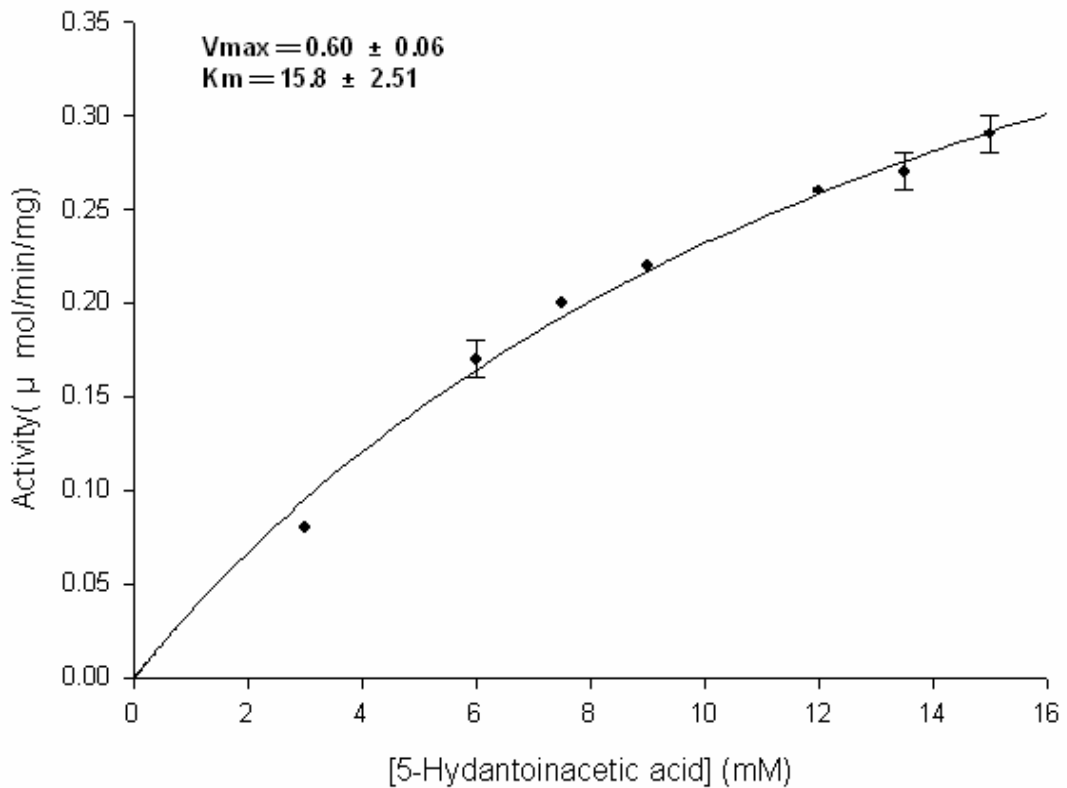
b. 3-Iminoisoindolinone



A2. Wavelength scan of a) Parabanic acid and b) 3-Iminoisoindolinone.

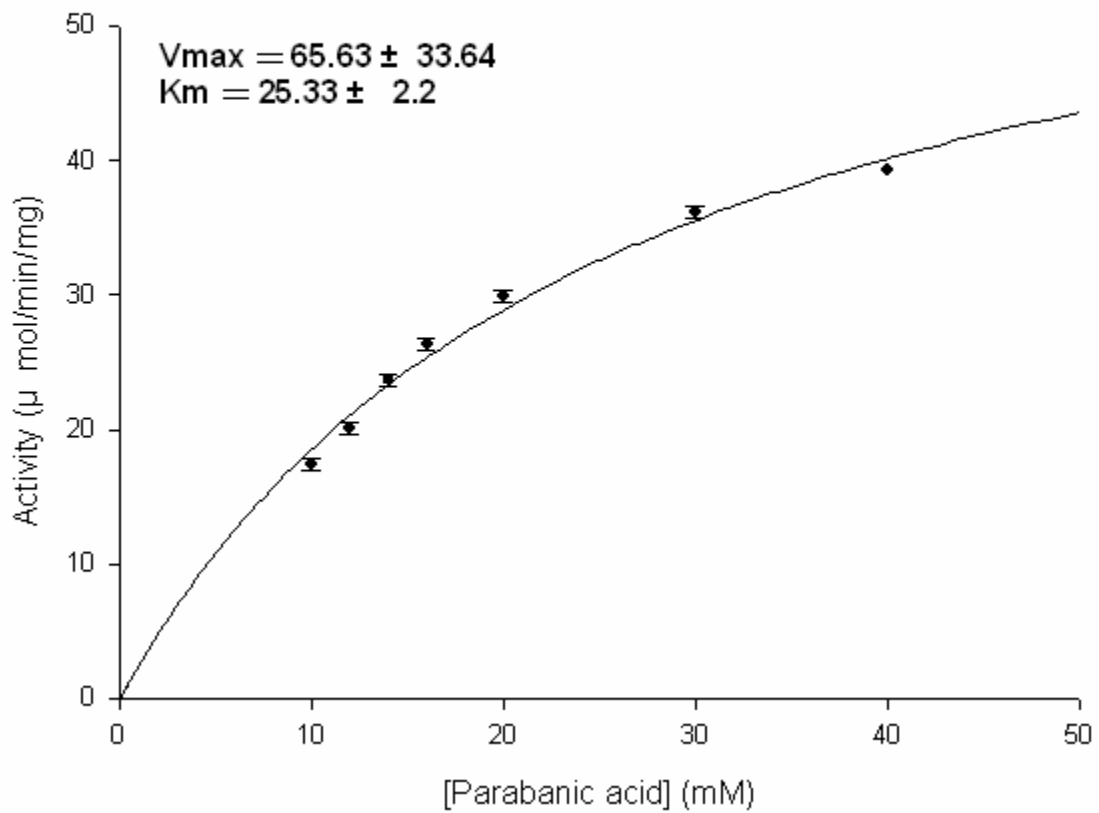
1) Substrate activity of parabanic acid were measured at 25°C in 100 mM Bis-Tris propane (pH 7). A change in A339 of 0.028 represents the hydrolysis of 1 mol of parabanic acid. 2) Inhibitory activity of parabanic acid was measured at 25°C in 100 mM Bis-Tris propane (pH 7) using 3-imoinisoindolinone as substrate. A change in A350 of 0.15 represents the hydrolysis of 1 mol of the substrate.

Michaelis-Menten



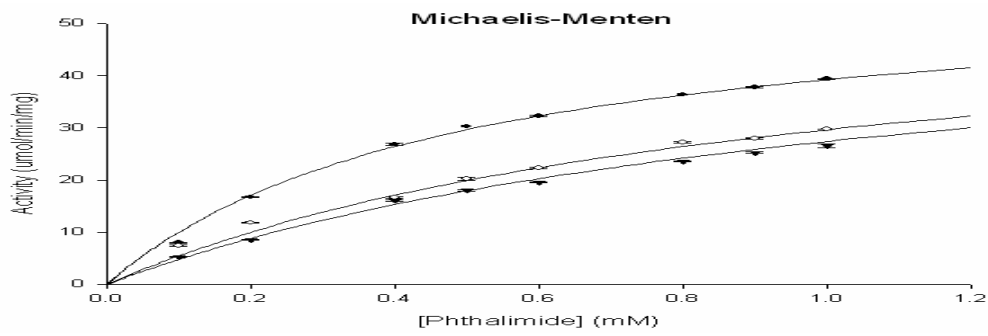
A3. Activity of *Agrobacterium tumefaciens* hydantoinase using 5-hydantoinacetic acid as substrate. Activity assay was measured at 25°C in 100 mM Bis-Tris propane(pH 7). A change in A240 of 0.1 represents the hydrolysis of 1 mol of 5-hydantoinacetic acid.

Michaelis-Menten

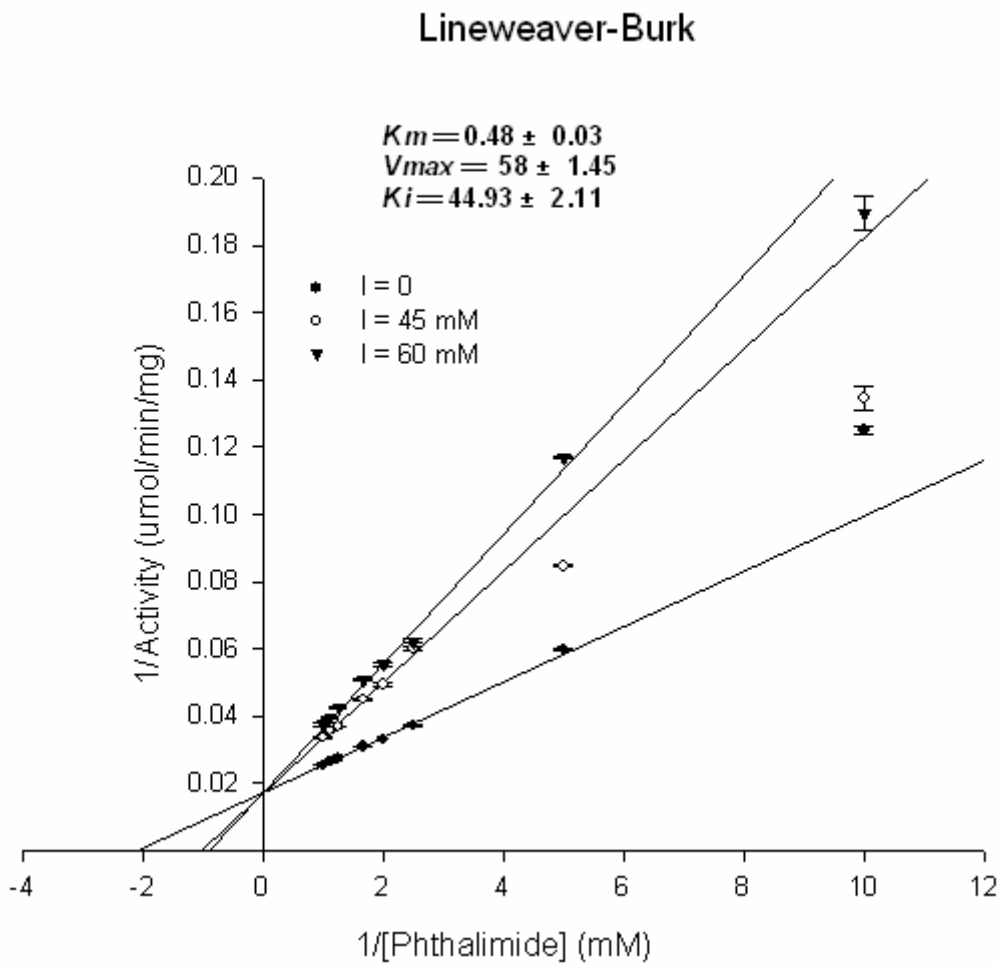


A4. Activity of *Agrobacterium tumefaciens* hydantoinase using Parabanic acid as substrate. Activity assay was measured at 25°C in 100 mM Bis-Tris propane (pH 7). A change in A339 of 0.028 represents the hydrolysis of 1 mol of parabanic acid

a.



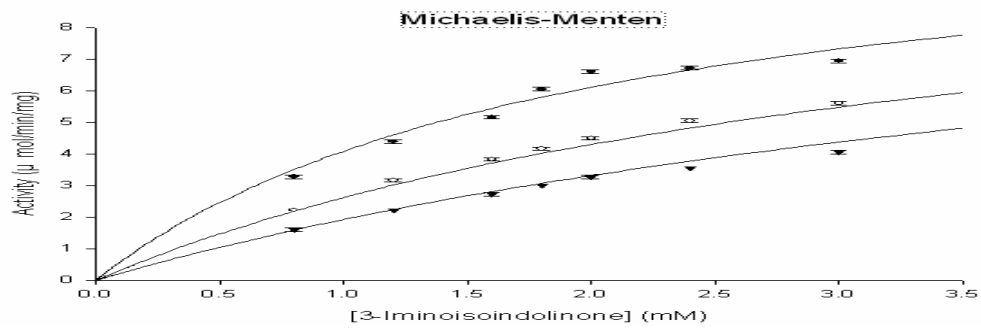
b.



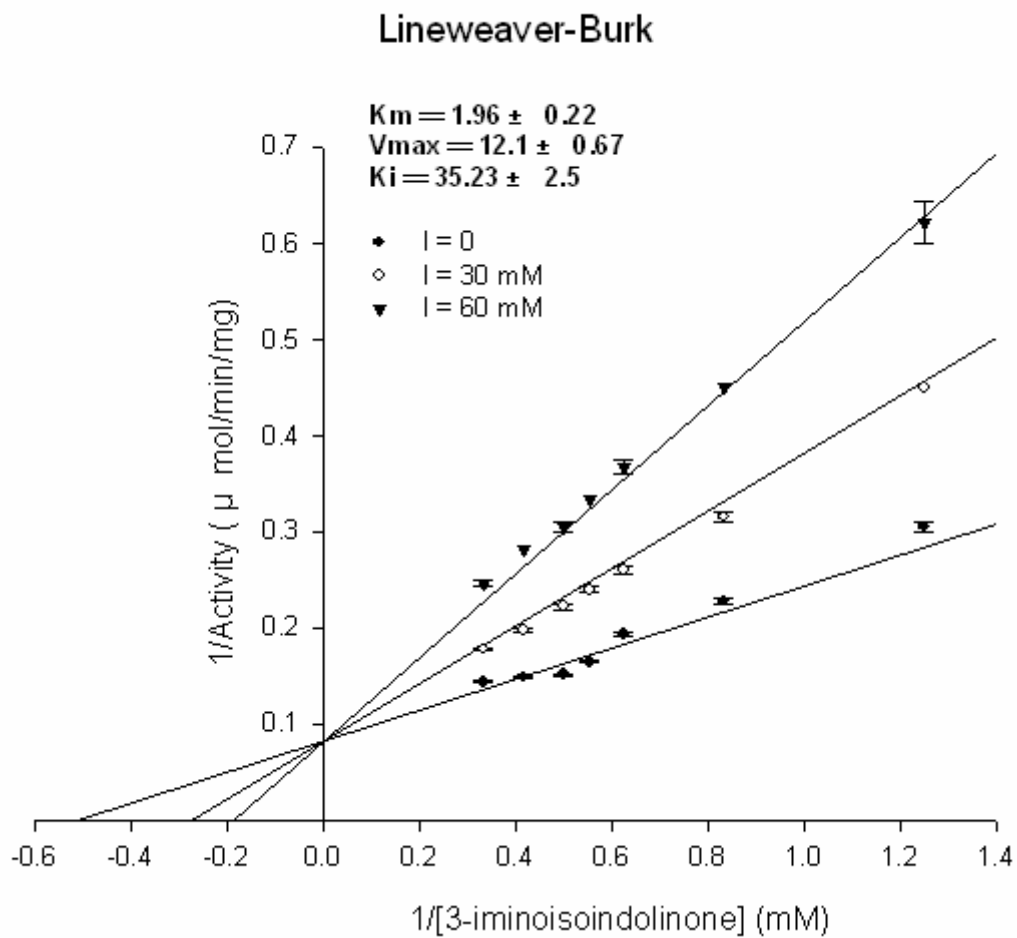
A5. 5-hydantoinacetic acid is a competitive inhibitor for *Oreochromis niloticus* imidase.

Inhibitory activity of 5-hydantoinacetic acid was measured at 25°C in 100 mM Bis-Tris propane at pH 7.0 using phthalimide as substrate. A change in A298 of 2.26 represents the hydrolysis of 1 mol of the substrate.

a.



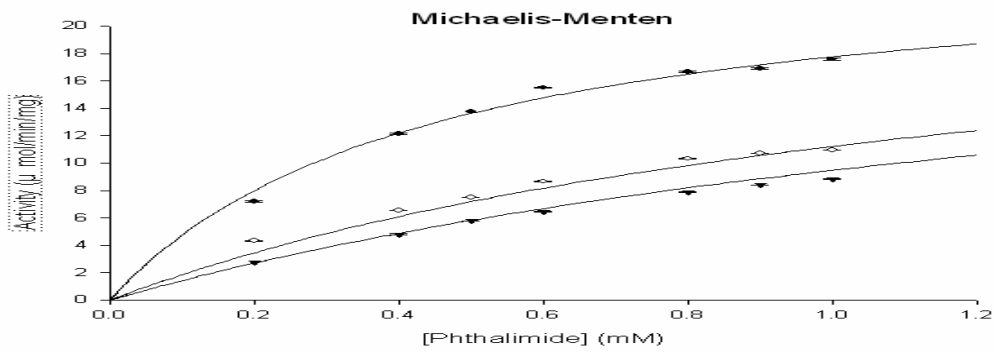
b.



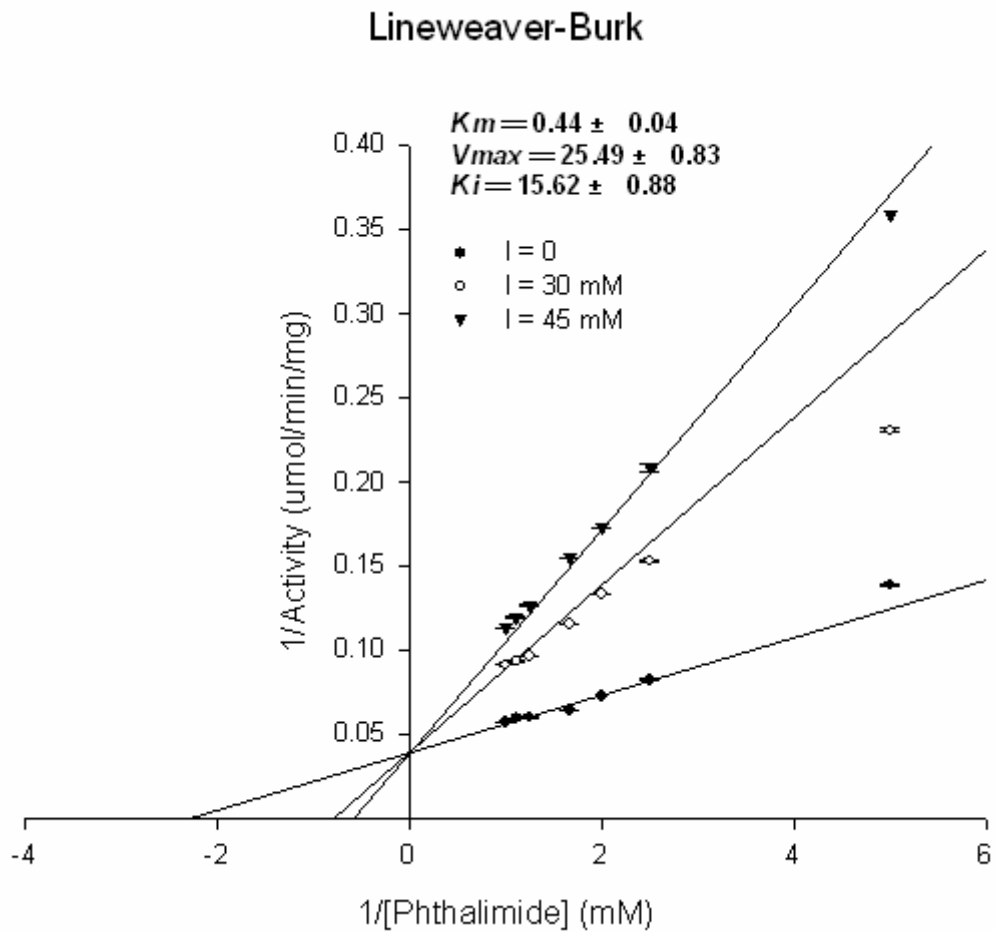
A6. Parabanic acid is a competitive inhibitor for *Oreochromis niloticus* imidase.

Inhibitory activity of parabanic acid was measured at 25°C in 100 mM Bis-Tris propane (pH 7) using 3-imoinisoindolinone as substrate. A change in A₃₅₀ of 0.15 represents the hydrolysis of 1 mol of the substrate.

a.



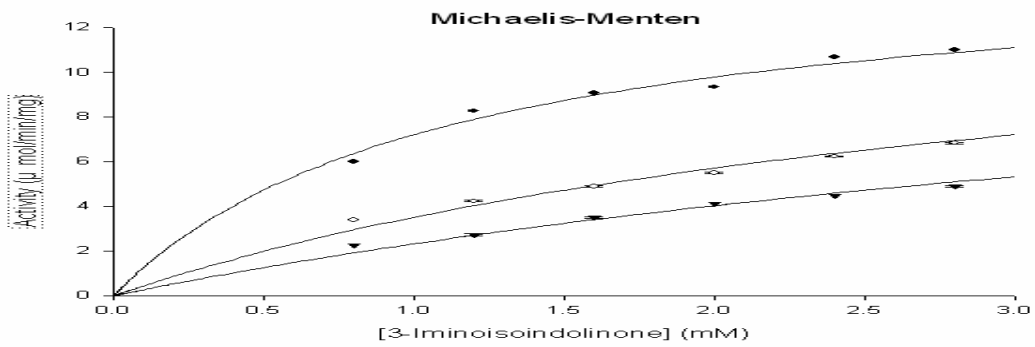
b.



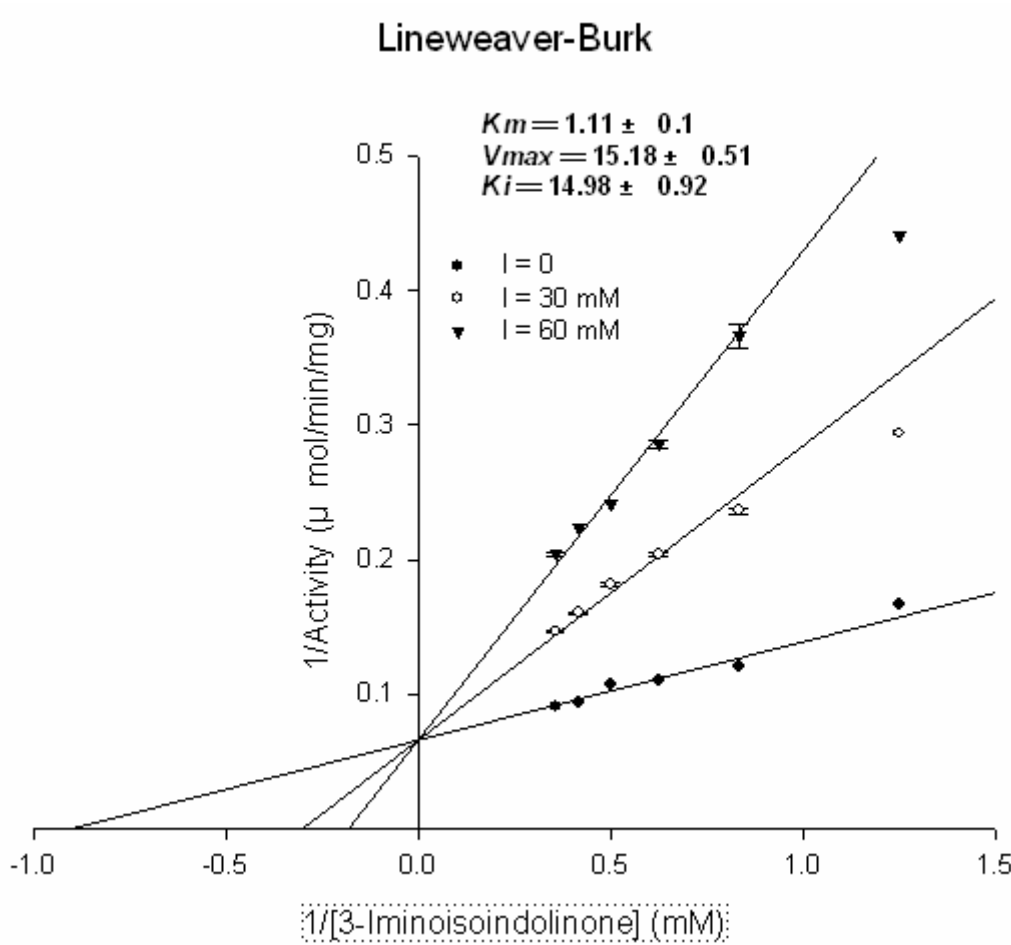
A5. 5- hydantoinacetic acid is a competitive inhibitor for pig liver imidase.

Inhibitory activity of 5-hydantoinacetic acid was measured at 25°C in 100 mM Bis-Tris propane at pH 7.0 using phthalimide as substrate. A change in A298 of 2.26 represents the hydrolysis of 1 mol of the substrate.

a.



b.



A6. Parabanic acid is a competitive inhibitor for pig liver imidase.

Inhibitory activity of parabanic acid was measured at 25°C in 100 mM Bis-Tris propane (pH 7) using 3-imoinisoindolinone as substrate. A change in A350 of 0.15 represents the hydrolysis of 1 mol of the substrate.